Article

The CDK8 Complex and Proneural Proteins Together Drive Neurogenesis from a Mesodermal Lineage

Highlights

- The generation of the *C. elegans* I4 neuron from mesoderm depends on HLH-3/Ascl1

- HLH-2/Tcf3 cooperates with HLH-3/Ascl1 to drive efficient I4 neurogenesis

- The Mediator Cdk8 kinase module acts genetically downstream of HLH-2/Tcf3

- Cdk8 kinase might promote I4 neurogenesis by inhibiting Cdk7/cyclin H function

Authors

Shuo Luo, H. Robert Horvitz

Correspondence

horvitz@mit.edu

In Brief

Luo and Horvitz report that the proneural basic-helix-loop-helix protein HLH-2/Tcf3 cooperates with HLH-3/Ascl1 to drive efficient generation of the I4 neuron from a mesodermal lineage in *C. elegans*. HLH-2 functions genetically through the Mediator Cdk8 kinase module, which might promote I4 neurogenesis by inhibiting Cdk7/cyclin H function.

CrossMark

CellPress

Article

CellPress

The CDK8 Complex and Proneural Proteins Together Drive Neurogenesis from a Mesodermal Lineage

Shuo Luo[1] and H. Robert Horvitz[1,2,*]
[1]Howard Hughes Medical Institute and Department of Biology, Massachusetts Institute of Technology, Cambridge, MA 02139, USA
[2]Lead Contact
*Correspondence: horvitz@mit.edu
http://dx.doi.org/10.1016/j.cub.2017.01.056

SUMMARY

At least some animal species can generate neurons from mesoderm or endoderm, but the underlying mechanisms remain unknown. We screened for *C. elegans* mutants in which the presumptive mesoderm-derived I4 neuron adopts a muscle-like cell fate. From this screen, we identified HLH-3, the *C. elegans* homolog of a mammalian proneural protein (Ascl1) used for in vitro neuronal reprogramming, as required for efficient I4 neurogenesis. We discovered that the CDK-8 Mediator kinase module acts together with a second proneural protein, HLH-2, and in parallel to HLH-3 to promote I4 neurogenesis. Genetic analysis revealed that CDK-8 most likely promotes I4 neurogenesis by inhibiting the CDK-7/CYH-1 (CDK7/cyclin H) kinase module of the transcription initiation factor TFIIH. Ectopic expression of HLH-2 and HLH-3 together promoted expression of neuronal features in non-neuronal cells. These findings reveal that the Mediator CDK8 kinase module can promote non-ectodermal neurogenesis and suggest that inhibiting CDK7/cyclin H might similarly promote neurogenesis.

INTRODUCTION

During bilaterian development, mesoderm and endoderm give rise to primarily non-neural tissues, whereas neurons are generated mostly from ectoderm. However, some animals, such as jellyfish and sea urchins, have subsets of neural cells derived from non-ectodermal origins, such as striated muscle and endoderm [1, 2]. It is not known whether the specification of non-ectodermal neural cells involves molecular mechanisms different from those of ectodermal neural specification. Also, because generating neurons from non-ectodermal cells is an important approach in neuroregenerative medicine, understanding molecular mechanisms underlying such neurogenesis might identify novel factors useful in regenerative medicine.

The nervous system of the *C. elegans* adult hermaphrodite consists of 302 neurons, 294 of which are derived from the AB blastomere, which primarily generates ectodermal cells [3]. By contrast, six pharyngeal neurons are generated from the MS blastomere, which generates mostly mesodermal cells (Figure 1A), and two neurons are generated from the C lineage, which generates both ectoderm and mesoderm. The MS-derived pharyngeal I4 neuron is generated from a progenitor cell that divides to give rise to I4 and a pharyngeal muscle cell [3]. Pharyngeal muscle cells are sometimes considered myoepithelial; however, these cells function as muscles, have molecular features characteristic of muscle cells, and their normal development depends on mesodermal transcription factors, so we view them as muscles [4, 5]. We hypothesized that I4 might overcome a mesodermal cell fate to become a neuron.

Here we report the identification of genetic mutants in which the I4 neuron adopts a muscle-like cell fate and show that two conserved genetic pathways, a proneural pathway and a Mediator pathway, act synergistically to promote I4 neurogenesis from mesoderm. We found that HLH-3, the homolog of a mammalian protein (Ascl1) that has been used extensively in neuronal reprogramming [6–8], HLH-2, and the evolutionarily conserved Mediator CDK8 kinase module promote I4 neurogenesis. Overexpression of HLH-2 and HLH-3 together promotes partial neuronal transformation of non-neuronal cells, including body-wall muscle cells. Our findings reveal that the CDK8 kinase module can promote non-ectodermal neurogenesis.

RESULTS

I4 Precursor Cells Transiently Express a Mesodermal Cell-Fate Reporter

We first investigated whether the I4 neuron expresses typical neuronal features by examining the expression of two broadly expressed neuronal reporters, for the small GTPase RAB-3 (*gfp::rab-3*) [9] and the guanine nucleotide exchange factor homolog RGEF-1 (P*rgef-1::dsRed*) [10], in I4. We observed that both reporters were expressed in I4 and other MS-derived neurons (Figure 1F; S.L., unpublished data); observations by Stefanakis et al. [11] similarly suggest that MS- and AB-derived neurons share basic neuronal molecular attributes. To determine whether I4 precursor cells express mesodermal characteristics, we examined the expression of an *hlh-1* reporter during embryogenesis. HLH-1 is the *C. elegans* homolog of the mammalian muscle master regulator MyoD and is expressed exclusively in myogenic lineages (Expression Patterns in *Caenorhabditis* [EPIC]; http://epic.gs.washington.edu). We found that I4 progenitor cells and the newly generated presumptive I4 cell were labeled by the HLH-1 reporter (Figure 1B). Our findings indicate that I4 precursor cells are at least to this extent mesodermal.

CrossMark
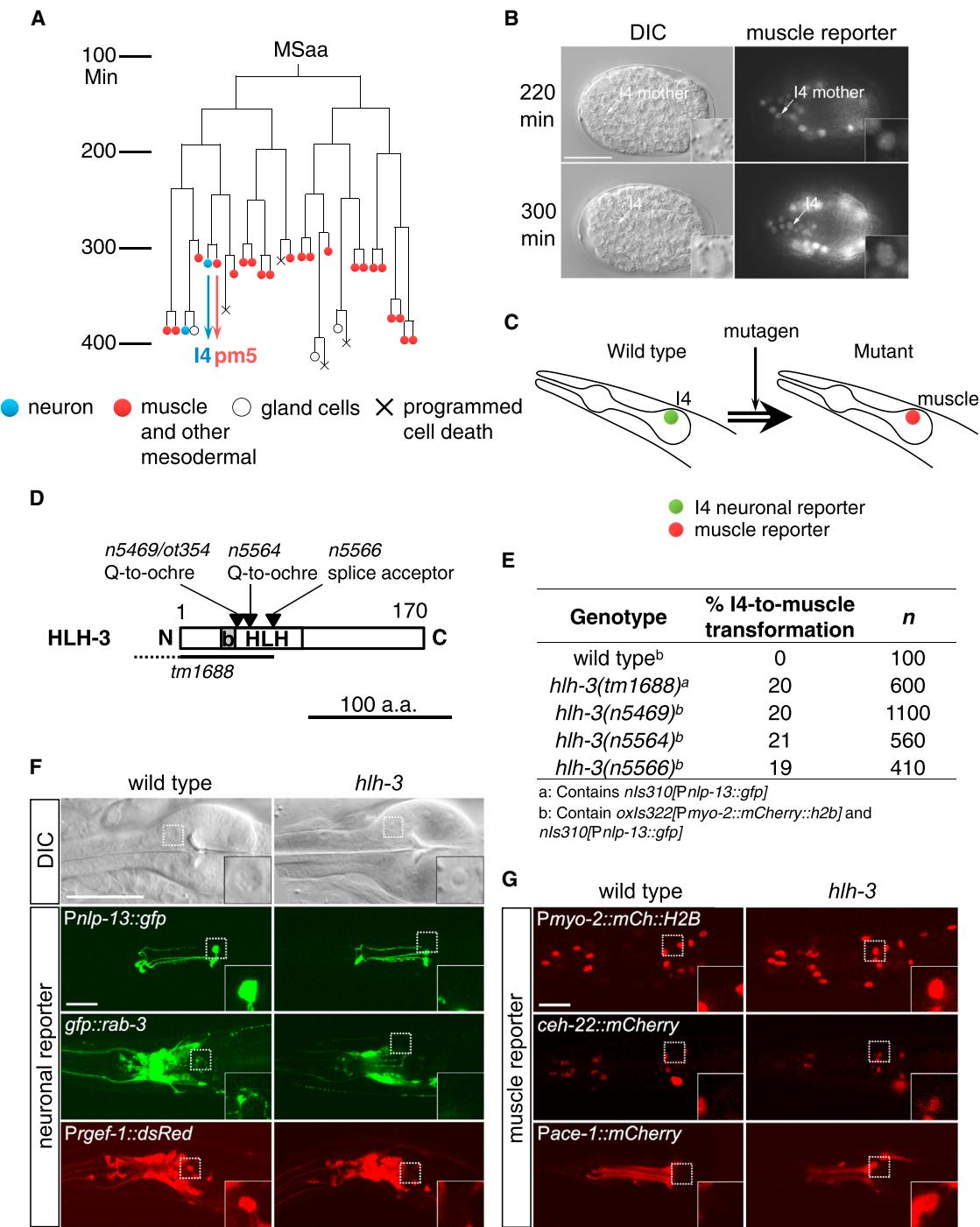
Figure 1. The Mesoderm-Derived I4 Neuron Adopts a Pharyngeal Muscle Cell Fate in *hlh-3* Mutants

(A) Diagram of the MSaa embryonic cell lineage, which generates the I4 neuron. Neuronal cells, blue; muscle and other mesodermal cells, red.

(B) A transcriptional reporter for the *C. elegans* MyoD gene *hlh-1* is expressed in the I4 mother cell and I4 during embryogenesis (arrows and insets).

(C) Schematic illustration of the genetic screen for mutants transformed in the I4 cell fate from neural to muscle.

(D) Schematic showing HLH-3 protein domains and mutations. b, basic domain; HLH, helix-loop-helix.

(E) HLH-3 mutants have partial defects in I4 neurogenesis.

(F) The I4 cell in an *hlh-3(n5469)* mutant adopts a non-neuronal fried-egg-like (in contrast to a neuronal speckled) nuclear morphology and does not express the I4 reporter P$_{nlp-13}$::*gfp* or the neuronal reporters P$_{rab-3}$::*gfp::rab-3* and P$_{rgef-1}$::*dsRed2* (boxes and insets).

(G) The I4 cell in *hlh-3* mutants expresses a pm5-specific reporter, P$_{ace-1}$::*mCherry*, as well as pharyngeal muscle reporters P$_{myo-2}$::*mCherry::H2B* and P$_{ceh-22}$::*ceh-22::mCherry*, none of which is expressed in wild-type I4 (boxes and insets).

Scale bars, 20 μm. See also Figure S1.

The I4 Neuron Adopts a Muscle-like Cell Fate in *hlh-3* Mutants

To seek mutants in which I4 adopts a muscle cell fate, we used a transgenic strain in which the I4 neuronal cell fate is labeled by the neural peptide reporter $P_{nlp-13}::gfp$ [12] and pharyngeal muscle cell fate is labeled by the pharyngeal myosin heavy-chain reporter $P_{myo-2}::mCherry::H2B$ [13]. We performed genetic screens and identified mutants that specifically lost I4 GFP expression (Figures 1C and 1F). Three such mutants carried alleles of the gene *hlh-3*, which encodes a basic-helix-loop-helix (bHLH) transcription factor homologous to the mammalian proneural protein Ascl1/Mash1 (Figures 1D and 1E). Ascl1 is involved in neural development in *Drosophila* and mammals, and overexpression of Ascl1 with other transcription factors drives reprogramming of various types of mesodermal and endodermal cells into neurons [6, 8, 14–16].

One *hlh-3* allele, *n5469*, contains an early stop codon that truncates the protein before the evolutionarily conserved HLH domain and most likely is a molecular null (Figure 1D). The I4 cell in *hlh-3* mutants appears to adopt a muscle-cell-like fate: (1) the nuclear morphology of I4 as visualized using Nomarski optics was transformed from a neuronal speckled morphology to a non-neuronal, fried-egg morphology (Figure 1F); (2) wild-type I4 expressed neuronal markers $P_{nlp-13}::gfp$, $P_{rab-3}::gfp::rab-3$, and $P_{rgef-1}::dsRed$, whereas none of these markers was expressed in the mutant presumptive I4 cell (Figure 1F); and (3) the mutant I4 cell expressed pharyngeal muscle reporters $P_{myo-2}::mCherry::His2B$ and $P_{ceh-22}::ceh-22::mCherry$ [4, 17] (Figure 1G). We found that the acetylcholine esterase reporter $P_{ace-1}::mCherry$, which normally labels the I4 sister cell pm5 [18], labeled an extra pm5 muscle cell in the *hlh-3* mutant pharynx (wild-type, n = 6 pm5; *hlh-3*, n = 7 pm5) (Figure 1G), indicating that the I4 cell in *hlh-3* mutants failed to be specified as a neuron and instead adopted the cell fate of its sister pm5 pharyngeal muscle cell. We were able to rescue the I4 defects by expressing a wild-type copy of the *hlh-3* gene in *hlh-3* mutants (Figure S1A).

HLH-3 Is Mostly Dispensable for Neurogenesis

Of the 20 neurons in the wild-type *C. elegans* pharynx, only I4 seemed to be affected by the disruption of HLH-3 (Figure S2C and data not shown). To further explore a possible role for HLH-3 in the neurogenesis of neurons other than I4, we scored the number of neurons expressing neurotransmitter reporter transgenes for cholinergic, GABAergic, glutamatergic, dopaminergic, serotonergic, and tyraminergic/octopaminergic neurons in *hlh-3* double mutants that also contained *hlh-2* or *dpy-22* mutations (we used the second mutation to sensitize the strain and potentially increase the magnitude of defects; see below); together, these reporters label about 240 of the 302 neurons in *C. elegans* (Figure S2A). We found that approximately 10% of wild-type I4 expressed the glutamate transporter transgene $P_{eat-4}::eat-4::mCherry$ (a fosmid-based translational fusion constructed by [19]) but none of the other reporters, indicating that I4 might be glutamatergic (Figure S2B). We did not find any significant difference in the number of *eat-4*-expressing neurons between the wild-type and *hlh-3* double-mutant animals, showing that the fates of most glutamatergic neurons were not altered (Figure S2D). (That I4 is transformed to a muscle cell in *hlh-3* mutants did not result in a lower count for *hlh-3* mutants,

because only 10% of wild-type I4s express the reporter.) We similarly observed no major differences in cholinergic, dopaminergic, serotonergic, or tyraminergic/octopaminergic neuron numbers between wild-type and *hlh-3* mutant animals (Figures S2E and S2G–S2I). By contrast, we noticed a mild deficit in GABAergic neuron number in *hlh-3* double mutants, which had one to five (mean 1.3) fewer GABAergic ventral cord motor neurons than did wild-type animals (Figure S2F). Further analysis indicated that this defect was most likely caused by the *hlh-2/3* mutation (data not shown). In mammals, knockout of Ascl1 results in impaired neurogenesis in confined neural regions, including the ventral telencephalon, olfactory bulb, and autonomic ganglia, whereas neurogenesis in other brain regions remains grossly normal [15, 20]. We conclude that, like Ascl1, its homolog HLH-3 promotes neurogenesis of I4 and a few GABAergic neurons but is not generally required for neurogenesis.

HLH-3 Is Expressed in the Newly Generated I4 Cell and Probably Functions Cell Autonomously

We used an HLH-3::GFP fusion protein to examine HLH-3 expression during embryogenesis. HLH-3::GFP was expressed in the I4 neuron shortly after its mother divided to generate I4; by contrast, the I4 sister, pm5, did not express this protein (Figure 2A). We also observed expression of HLH-3::GFP in multiple AB-derived neural precursors (data not shown). The broad expression of HLH-3::GFP was mostly confined to embryos and was no longer detectable in the I4 neuron in newly hatched L1s (larval stage 1; Figure S1B), suggesting that *hlh-3* functions primarily in early embryos to promote I4 specification. To determine whether HLH-3 functions within the I4 lineage or in neighboring cells to promote I4 neurogenesis, we used a laser microbeam to selectively kill the cells that make direct contact with I4 progenitor cells during embryogenesis (Figure 2B). We asked whether elimination of any neighboring cells impairs I4 neurogenesis. Laser ablation of the founder cells AB, P2, and E, which normally generate neighbors of I4 progenitor cells in early embryos, did not affect I4 GFP reporter expression (Figure 2C). By contrast, killing the I4 progenitor cell EMS eliminated I4 GFP reporter expression (Figure 2C). These results suggest that HLH-3 most likely functions cell autonomously to drive I4 neurogenesis.

HLH-2, the *C. elegans* Homolog of Daughterless/Tcf3, Functions Synergistically with HLH-3 to Promote Efficient I4 Neurogenesis

The neurogenesis of I4 is only partially disrupted in the absence of functional HLH-3: about 80% of *hlh-3* null mutants (*n5469* and *tm1688*) still generate an I4 neuron (Figures 1D and 1E). Thus, other genes probably function in addition to *hlh-3* to drive I4 neurogenesis. HLH-3 can interact and form heterodimers with another bHLH transcription factor, HLH-2, the *C. elegans* homolog of the conserved E2A/Tcf3/Daughterless protein [21, 22]. Tcf3 and Daughterless are broadly expressed in developing neural precursors in vertebrates and *Drosophila*, respectively, and disruption of either protein results in loss of neural tissues and aberrant morphogenesis [22–25]. Using a reporter transgene that expresses an HLH-2::GFP fusion protein [26], we found that HLH-2::GFP was expressed in the I4 neuron shortly after
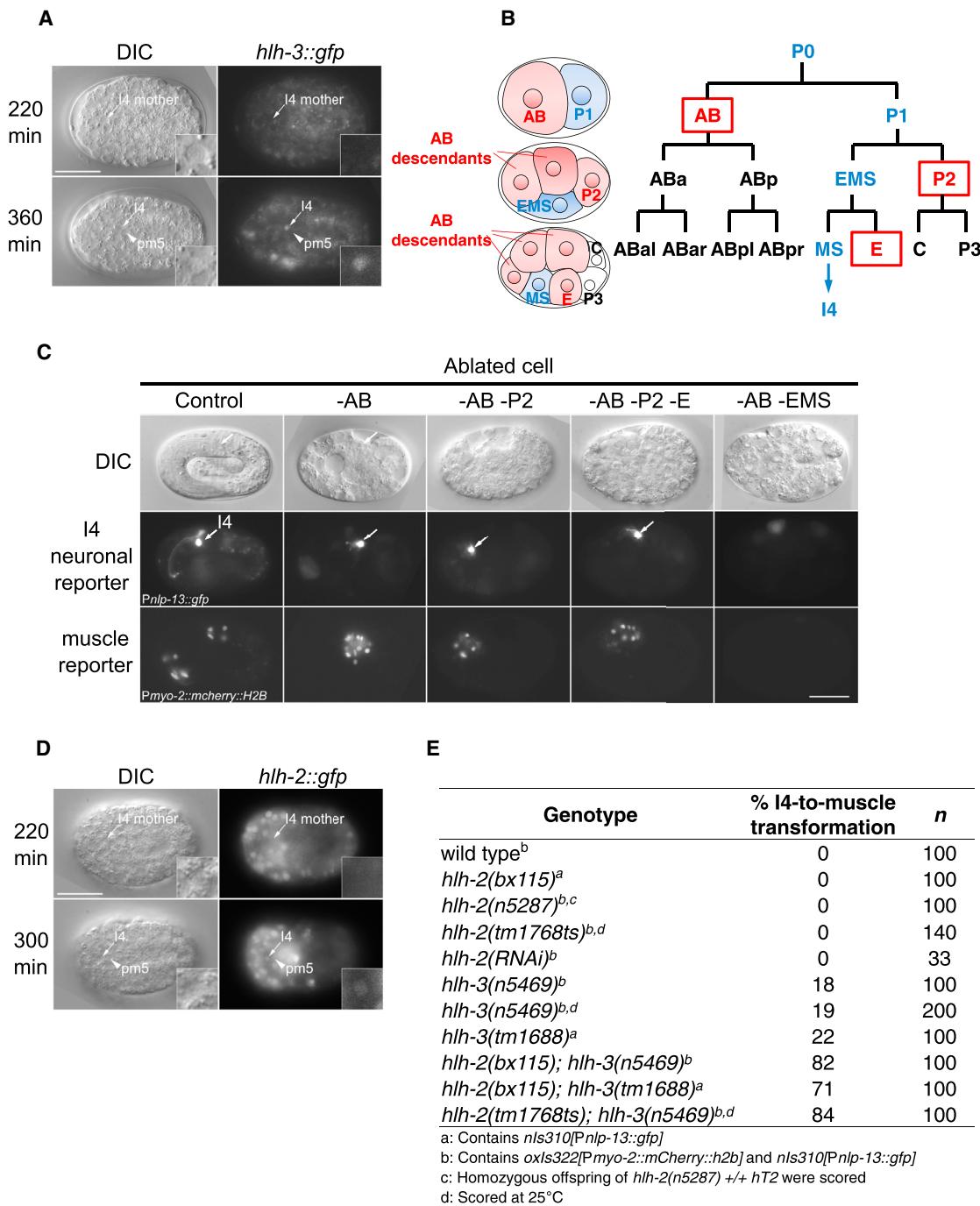
Figure 2. HLH-3 Functions Cell Autonomously and Synergistically with HLH-2 to Promote I4 Neurogenesis

(A) An HLH-3::GFP fusion protein is expressed in wild-type I4 (arrows and insets), but not in its sister pm5 (arrowheads), shortly after their generation.

(B) Diagram of the first several embryonic cell divisions in wild-type embryos, with I4 and the I4 progenitors shown in blue and the I4-neighboring progenitors boxed and shown in red.

(C) Laser ablation of AB, P2, and E does not affect I4 reporter P$_{nlp-13}$::gfp expression (arrows). By contrast, ablation of EMS (which generates I4) eliminates P$_{nlp-13}$::gfp expression. Number of embryos: –AB, n = 5; –AB–P2, n = 3; –AB–P2–E, n = 3; –AB–EMS, n = 1.

(D) An HLH-2::GFP fusion protein is specifically expressed in wild-type I4 (arrows and insets), but not in its sister pm5 (arrowheads), shortly after their generation.

(E) Even though a null allele of hlh-2, n5287, does not disrupt I4 development (possibly because of a maternal contribution of HLH-2 to arrested homozygotes), introducing weaker hlh-2 alleles into an hlh-3 null mutant (n5469 or tm1688) significantly enhances I4 misspecification.

Scale bars, 20 μm. See also Figures S1–S3.

The table in panel E:

Genotype	% I4-to-muscle transformation	n
wild type[b]	0	100
hlh-2(bx115)[a]	0	100
hlh-2(n5287)[b,c]	0	100
hlh-2(tm1768ts)[b,d]	0	140
hlh-2(RNAi)[b]	0	33
hlh-3(n5469)[b]	18	100
hlh-3(n5469)[b,d]	19	200
hlh-3(tm1688)[a]	22	100
hlh-2(bx115); hlh-3(n5469)[b]	82	100
hlh-2(bx115); hlh-3(tm1688)[a]	71	100
hlh-2(tm1768ts); hlh-3(n5469)[b,d]	84	100

a: Contains nIs310[Pnlp-13::gfp]
b: Contains oxIs322[Pmyo-2::mCherry::h2b] and nIs310[Pnlp-13::gfp]
c: Homozygous offspring of hlh-2(n5287) +/+ hT2 were scored
d: Scored at 25°C

its generation but was absent from its sister cell, pm5 (Figure 2D). Also like HLH-3::GFP, HLH-2::GFP was broadly expressed in early embryos but was not detectable in most neurons, including I4 in newly hatched L1s (Figure S1B), suggesting that *hlh-2* most likely functions in early embryos to promote I4 specification. We then asked whether HLH-2 is required for I4 neurogenesis. Both *hlh-2(n5287)* null mutants and animals treated with *hlh-2* RNAi displayed embryonic lethality; nonetheless, we did not observe obvious defects in I4 GFP expression (we note that in both cases maternal HLH-2 was still likely to be present) (Figure 2E; Figure S1C). By contrast, the introduction of an *hlh-2* partial loss-of-function allele (*bx115* or *tm1768*) into an *hlh-3* null background significantly enhanced I4 misspecification, and in about 80% of *hlh-2; hlh-3* double mutants the I4 cell adopted a muscle-like cell fate (Figure 2E). Given this genetic enhancement, we conclude that HLH-2 functions to promote I4 neurogenesis at least partly through a genetic pathway that acts in parallel to HLH-3.

Multiple bHLH Proneural Proteins Promote MS Neurogenesis

The *C. elegans* genome encodes 42 bHLH factors, with multiple bHLH proteins able to form dimers with HLH-2 (Figure S3A) [21]. We tested whether any of the proneural bHLH proteins, including neurogenin NGN-1 and NeuroD CND-1, are required for I4 neurogenesis. Examination of the I4 neuron in either *ngn-1* or *cnd-1* single mutants or *hlh-2; ngn-1* or *hlh-2; cnd-1* double mutants using the reporter transgene P*nlp-13*::*gfp* did not reveal any defects in I4 neurogenesis (Figure S3B). Furthermore, we did not observe defects in I4 neurogenesis in *hlh-4*, *6*, *10*, *12*, *13*, *15*, *19*, or *lin-32* mutant animals using both Nomarski optics and the pan-neuronal reporter transgene P*rgef-1*::*dsRed*, suggesting that I4 neurogenesis is specifically dependent on HLH-3 and not on other HLH-2-interacting bHLH proteins (Figures S3E–S3L). However, *ngn-1* and *cnd-1* mutants were disrupted in the neurogenesis of other MS-derived neurons: around 40% of *ngn-1* mutant animals lacked the M1 neuron, and in 25% of *cnd-1* mutant animals the I3 neuron adopted a gland cell fate (the cell fate of its sister cell) (Figures S3C and S3D). These results indicate that the generation of mesoderm-derived neurons in *C. elegans* involves multiple bHLH proneural proteins, with I4 neurogenesis depending specifically on HLH-3 (Figure 3E).

Mediator Subunits Function in the HLH-2 Pathway to Promote I4 Neurogenesis

To search for additional factors that function with HLH-2 and HLH-3 to promote efficient I4 neurogenesis, we examined other mutant isolates from our screens. We found that five mutants carry alleles of *dpy-22*, and two carry alleles of *let-19* (Figure 3A; Figure S4A). Like *hlh-3* mutations, mutations in *dpy-22* and *let-19* disrupted I4 specification, and the I4 cell adopted a pharyngeal muscle cell fate (Figure 3B). *dpy-22* and *let-19* encode the worm homologs of the evolutionarily conserved Mediator subunits Med12 and Med13, respectively. Mediator is a multi-subunit complex that bridges DNA-binding proteins (transcription factors/coactivators) with the RNA polymerase II transcription machinery and is involved in many aspects of gene regulation and animal development [27–29]. Med12 disruption in mice and zebrafish results in impaired development of the neural

crest and of non-ectodermal tissues, including heart and gut [30–32]. We found that although disruption of LET-19 function in the *let-19* mutant *n5470* also led to low-frequency (~3%, n = 60) neurogenesis defects of the M1 neuron (Figure 3C), disruption of DPY-22 in all five *dpy-22* mutants specifically disrupted I4 neurogenesis (Figure 3D). Because promoter-fusion reporter transgenes for *dpy-22* and *let-19* revealed broad GFP expression in developing embryos (Figure 4A), we conclude that DPY-22 and LET-19 most likely cooperate with cell-specific factors to drive I4 neurogenesis.

Further analysis revealed that the two *let-19* alleles contain missense mutations, and all five *dpy-22* alleles contain nonsense mutations that truncate the C-terminal PQ-rich domain (Figure 3A). Because none of these mutations is obviously null, we performed *dpy-22* or *let-19* RNAi to further reduce gene function in *dpy-22* and *let-19* mutants, respectively. We did not observe significant enhancement of the I4 misspecification (Figure S4B). In addition, we used cell-specific RNAi to express *dpy-22* or *let-19* siRNA under the *nlp-13* promoter (which is active only after I4 is generated; S.L., unpublished data) [33]. I4 appeared normal in position and morphology (Figures S4C and S4D), suggesting that Mediator is dispensable for the maintenance of the I4 cell fate after mid-late embryogenesis.

In vertebrates, Med12 interacts with transcription factors through its PQ-rich domain to promote gene expression and tissue development [34, 35]. To determine whether Mediator might promote I4 neurogenesis by interacting with bHLH proneural factors, we performed a yeast two-hybrid assay. We found that the DPY-22 PQ-rich domain selectively interacted with HLH-2 but not HLH-3, whereas the last 129 amino acids truncated in all five *dpy-22* alleles were required for this interaction (Figure 4B). Further analysis indicated that the PQ-rich domain interacted with the N-terminal half of HLH-2, the region of a predicted transactivation domain important for gene expression and neurogenesis [36, 37] (Figure 4C). These findings suggest that Mediator physically interacts with and might function in the same pathway as HLH-2 to promote I4 neurogenesis.

To test this hypothesis, we constructed Mediator and bHLH double mutants. All of the *dpy-22* and *let-19* single mutants showed a low frequency of I4 misspecification, and *dpy-22* or *let-19* RNAi in *dpy-22* or *let-19* mutants, respectively, did not significantly enhance I4 defects (Figures S4A and S4B). Introducing an *hlh-2* partial loss-of-function allele into *dpy-22* or *let-19* mutants also did not enhance I4 misspecification (Figure 4D). By contrast, disruption of *dpy-22* or *let-19* in an *hlh-3* null (*n5469*) background significantly enhanced I4 misspecification, with 77% and 55% of the I4 cells adopting a muscle cell fate, respectively (*let-19* and *hlh-3* are tightly linked, and thus *let-19* was tested using RNAi) (Figure 4E), indicating that Mediator and HLH-2 act together and in parallel to HLH-3 to promote I4 neurogenesis.

CDK-8 Probably Promotes I4 Neurogenesis by Inhibiting CDK-7/CYH-1

Med12 and Med13 are components of a four-protein Mediator kinase module, with the other two proteins being the cyclin-dependent kinase CDK8 and cyclin C [27, 28]. CDK8 is involved in cell-fate transformation during tumor generation and progression [38, 39]. To investigate whether the *C. elegans* counterparts
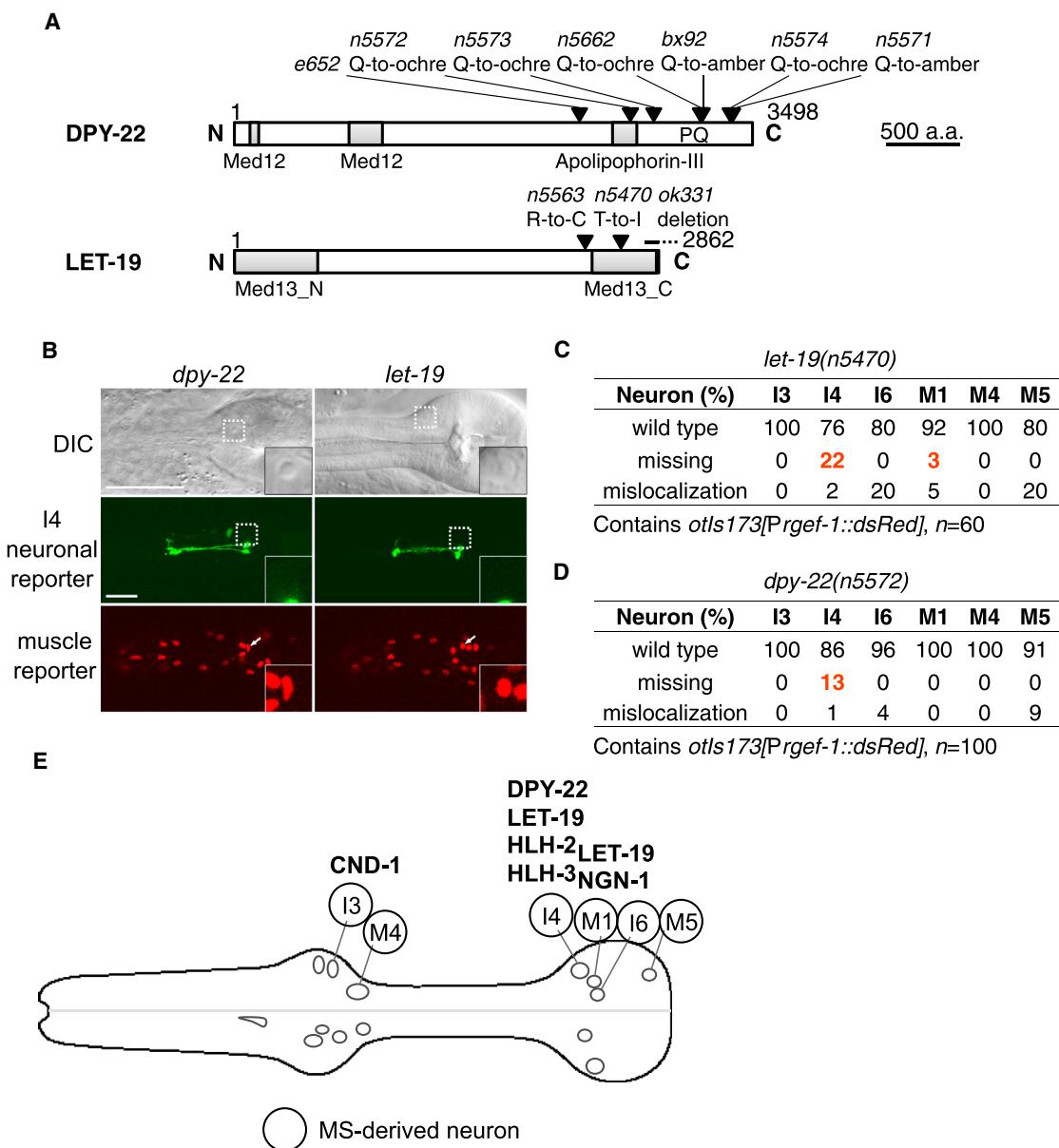
Figure 3. Disruption of the Mediator Subunits LET-19 and DPY-22 Leads to I4 Misspecification

(A) Schematics showing DPY-22 and LET-19 protein domains and mutations.

(B) The I4 cell in *dpy-22* and *let-19* mutants adopts a non-neuronal, fried-egg-like nuclear morphology and expresses the pharyngeal muscle reporter transgene P*myo-2*::mCherry::H2B, but not the I4 neuronal reporter transgene P*nlp-13*::*gfp* (boxes, arrows, and insets).

(C) *let-19* mutants have impaired neurogenesis of the I4 and M1 neurons (red).

(D) *dpy-22* mutants that lack the C-terminal PQ-rich domain have impaired neurogenesis of the I4 neuron (red).

(E) Diagram showing the requirement of bHLH and Mediator proteins for the expression of a neuronal cell fate of the MS-derived neurons. Mislocalization: M5, dorsal right (rather than dorsal left); M1, abnormally anterior; I6, abnormally dorsal medial (rather than dorsal left); I4, abnormally ventral, i.e., closer to the M2 neuron.

Scale bars, 20 μm. See also Figure S4.

of CDK8 and cyclin C are involved in I4 neurogenesis, we examined I4 development in *cdk-8(tm1238)* (CDK8) and *cic-1(tm3740)* (cyclin C) mutants. Both mutants contain substantial deletions of coding exons and both are most likely null (Figure S5A). *cdk-8* and *cic-1* single mutants had only very mild (<1%) defects in I4 neurogenesis (Figure S5B). Introducing a *cdk-8* or *cic-1* allele into a Mediator (*dpy-22*) or *hlh-2* mutant did not enhance I4 misspecification (Figure S5B). By contrast, disrupting *cdk-8* or *cic-1* in the *hlh-3(n5469)* null mutant substantially enhanced I4 misspecification, with 36% of the I4s in *hlh-3; cic-1* mutants and 48% of the I4s in *cdk-8; hlh-3* mutants adopting a muscle cell fate (Figure 5A). Because introduction of the *cdk-8* null allele into *cnd-1*

Panel D

Genotype	% I4-to-muscle transformation	n
wild type[b]	0	100
hlh-2(bx115)[a]	0	100
let-19(n5470)[b]	11	100
dpy-22(n5572)[b]	4	200
hlh-2(bx115); let-19(n5470)[b]	14	100
hlh-2(bx115); dpy-22(n5572)[b]	7	200

a: Contains nIs310[Pnlp-13::gfp]
b: Contains oxIs322[Pmyo-2::mCherry::h2b] and nIs310[Pnlp-13::gfp]

Panel E

Genotype[a]	% I4-to-muscle transformation	n
wild type	0	100
hlh-3(n5469)	21	100
dpy-22(n5572)	5	100
let-19(n5470)	16	200
hlh-3(n5469); dpy-22(n5572)	77	100
hlh-3(n5469); let-19(RNAi)	55	100

a: Contains oxIs322[Pmyo-2::mCherry::h2b] and nIs310[Pnlp-13::gfp]

Figure 4. The Mediator Subunits DPY-22 and LET-19 Function in the Same Pathway as HLH-2 and in Parallel to HLH-3 to Promote I4 Neurogenesis

(A) A GFP reporter transgene driven by the dpy-22 or let-19 promoter is expressed ubiquitously in developing embryos.

(B) Yeast two-hybrid assays showing that the DPY-22 PQ-rich domain interacts with HLH-2 (shown by the yeast growth on the –Leu–Trp–His–Ade quadruple-dropout plates). The C-terminal 129 amino acids are required for this interaction. Δ129, last 129 amino acids deleted; c129, only last 129 amino acids; BD, bait vector control; AD, prey vector control; SD, synthetic dropout.

(C) The DPY-22 PQ-rich domain interacts with the N terminus of HLH-2. Abbreviations are as in (B).

(D) Introducing the hlh-2 partial loss-of-function allele bx115 into dpy-22 or let-19 mutants does not enhance I4 misspecification.

(E) Disruption of dpy-22 or let-19 in the hlh-3 null mutant n5469 significantly enhances I4 misspecification.

Scale bar, 20 μm.

---

or ngn-1 single mutants did not enhance the frequency of I3 or M1 misspecification (Figures S3C, S3D, S5C, and S5D), we conclude that CDK-8 functions together with DPY-22 and HLH-2 and in parallel to HLH-3 to specifically promote I4 neurogenesis.

The enhanced I4 misspecification of cdk-8; hlh-3 double mutants could be fully rescued with a wild-type, but not a kinase-dead, CDK-8 cDNA, suggesting that the kinase activity of CDK-8 is required for promoting I4 neurogenesis (Figure 5B). We noticed that the penetrance of I4 misspecification in cdk-8; hlh-3 mutants (∼40%) was only about half of that in hlh-3; dpy-22 (∼80%) mutants; we speculate that DPY-22 functions only partially through CDK-8 and CIC-1, with other unidentified proteins downstream of DPY-22 acting in parallel to CDK-8 to promote I4 neurogenesis.

We then investigated what molecules act downstream of CDK-8 to promote I4 neurogenesis. Mammalian CDK8 phosphorylates several substrates, including serine 10 of histone 3 (H3S10) [40, 41] and the Notch protein [42]. H3S10 phosphoryla-

tion promotes the opening of chromatin structure by dissociating heterochromatin protein HP1 from trimethylated H3K9 (H3K9me3) [43–45], and Notch phosphorylation by CDK8 leads to degradation of the Notch intracellular domain [42]. We observed reduced H3S10 phosphorylation in cdk-8; hlh-3 double mutants; this reduction was rescued by expressing a wild-type, but not a kinase-dead, cdk-8 transgene (Figure S5E). However, overexpression of a phosphomimetic form of the replication-independent His3.3 protein HIS-71 (but not of a replication-dependent His3.1 protein, HIS-9) only partially suppressed the I4 misspecification of cdk-8; hlh-3 mutants (Figure S5F). We did not observe a significant effect of Notch disruption on I4 neurogenesis in wild-type or hlh-3 or cdk-8; hlh-3 mutants (Figures S6E–S6G). These observations suggested that CDK-8 might function primarily through one or more other mechanisms.

Mammalian CDK8 phosphorylates cyclin H on serines 5 and 304 and suppresses CDK7/cyclin H-activated gene transcription [46]. Serine 5 of cyclin H is completely conserved from C. elegans
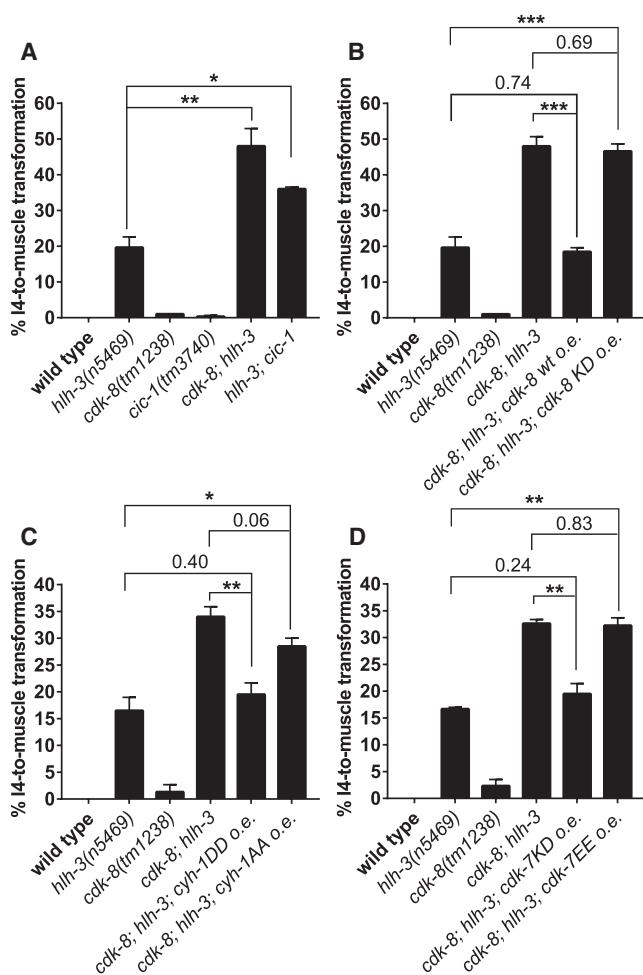
Figure 5. CDK-8 Functions in Parallel to HLH-3 to Promote I4 Neurogenesis, Possibly by Inhibiting CYH-1 and CDK-7

(A) Disruption of *cdk-8* or *cic-1* in the *hlh-3* null mutant *n5469* enhances I4 misspecification.

(B) Expressing a wild-type (WT), but not a kinase-dead (KD), copy of *cdk-8* cDNA using the *dpy-22* promoter rescues I4 misspecification in *cdk-8; hlh-3* double mutants.

(C) Overexpression of phosphomimetic CYH-1DD, but not non-phosphorylatable CYH-1AA, using the *dpy-22* promoter suppresses I4 defects in *cdk-8; hlh-3* mutants.

(D) Overexpression of kinase-dead CDK-7KD, but not phosphomimetic CDK-7EE, using the *dpy-22* promoter rescues I4 defects in *cdk-8; hlh-3* mutants.

o.e., overexpression. Mean ± SEM. *p < 0.05, **p < 0.01, ***p < 0.001 by Student's t test. See also Figures S5 and S6.

to mammals, whereas mammalian S304 is probably equivalent to *C. elegans* S327. We asked whether cyclin H might be a primary mediator of CDK-8 function. Overexpression of phosphomimetic (S5D S327D; "DD") CYH-1 cyclin H protein rescued I4 misspecification in the *cdk-8; hlh-3* mutant, whereas overexpression of a non-phosphorylatable (S5A S327A; "AA") CYH-1 protein did not rescue (Figure 5C), indicating that CDK-8 might promote I4 neurogenesis through inhibiting cyclin H. Because phosphorylation of cyclin H inhibits CDK7 kinase activity in the general transcription factor complex TFIIH [46], we tested whether mutations that either enhance or reduce CDK7 kinase

activity affect the *cdk-8; hlh-3* mutant phenotype. We found that overexpression of a kinase-dead version of CDK-7, K34A [47], resulted in full rescue of the *cdk-8; hlh-3* mutant phenotype, whereas overexpression of a constitutively active mutant of CDK-7, S157E T163E ("EE"; T loop double mutations) [47], did not have such an effect (Figure 5D). Our findings indicate that CDK-8 possibly promotes I4 neurogenesis by inhibiting CDK-7/cyclin H function and that H3S10 phosphorylation might also contribute to I4 specification (Figure 7).

Ectopic Expression of HLH-2 and HLH-3 Induces Partial Cell-Fate Transformation of Muscle Cells

To investigate whether the genes we identified are sufficient to induce the cell-fate transformation of presumptive muscle cells to an I4-like fate, we generated transgenic strains that stably express HLH-2, HLH-3, or both using the heat shock promoter $P_{hsp-16.2}$ [48]. We found that ectopic expression of HLH-2 and HLH-3 together (but not of either alone) by heat shock induced expression of a pan-neuronal reporter, $P_{rab-3}::gfp::rab-3$, in several body-wall muscle cells in 30% of heat-shocked animals (n = 10) (Figure 6A). In an independent experiment, 13% of heat-shocked animals (n = 15) expressed both pan-neuronal reporters $P_{rab-3}::gfp::rab-3$ and $P_{rgef-1}::dsRed$ in body-wall muscle and hypodermal cells, indicating that these non-neuronal cells indeed exhibit neuronal characteristics (Figure 6B). The affected muscle cells displayed neuron-like long processes but retained the muscle-like fried-egg morphology of their nuclei (Figures 6A and 6B), suggesting a partial cell-fate transformation. By contrast, overexpression of HLH-2 or HLH-3 alone or of HLH-2 and HLH-3 together did not eliminate *myo-2* reporter expression in pharyngeal muscle cells, including pm5 (data not shown), nor did it induce ectopic expression of the muscle reporter $P_{myo-3}::gfp$ or the intestinal reporter $P_{elt-2}::gfp$ (Figures 6C and 6D). Together, these observations indicate that the combined overexpression of HLH-2 and HLH-3 in L1 larvae drives a partial but specific neuronal cell-fate transformation of non-neuronal (body-wall muscle and hypodermal) cells.

Adult somatic cells in *C. elegans* might be more refractory to transcription factor-induced cell-fate transformation than cells in younger individuals [49]. We asked whether the ectopic expression of HLH proteins is more efficient in inducing cell-fate transformation in early embryos than in L1 larvae. Overexpression of HLH-2 and HLH-3 in combination or HLH-2 alone (but not HLH-3 alone) during early embryogenesis induced the generation of multiple cells that express the I4 reporter $P_{nlp-13}::gfp$, and in the case of HLH-3 the cells developed long processes, suggesting that HLH-2 is sufficient to induce ectopic I4-like neurogenesis and that HLH-3 might promote neuronal maturation (Figure 6E). We were unable to determine whether the extra I4-like cells were transformed from pm5 pharyngeal muscle cells or from any other mesodermal cells, as the heat-shocked embryos arrested development. Nevertheless, HLH-2 and HLH-3 overexpression did not eliminate all pharyngeal muscle reporter $P_{myo-2}::mCherry::H2B$ expression (Figure 6E), suggesting that HLH overexpression does not induce transformation of all mesodermal cells. Our findings indicate that the expression of HLH-2 and HLH-3 in early embryos can induce ectopic I4 neurogenesis.
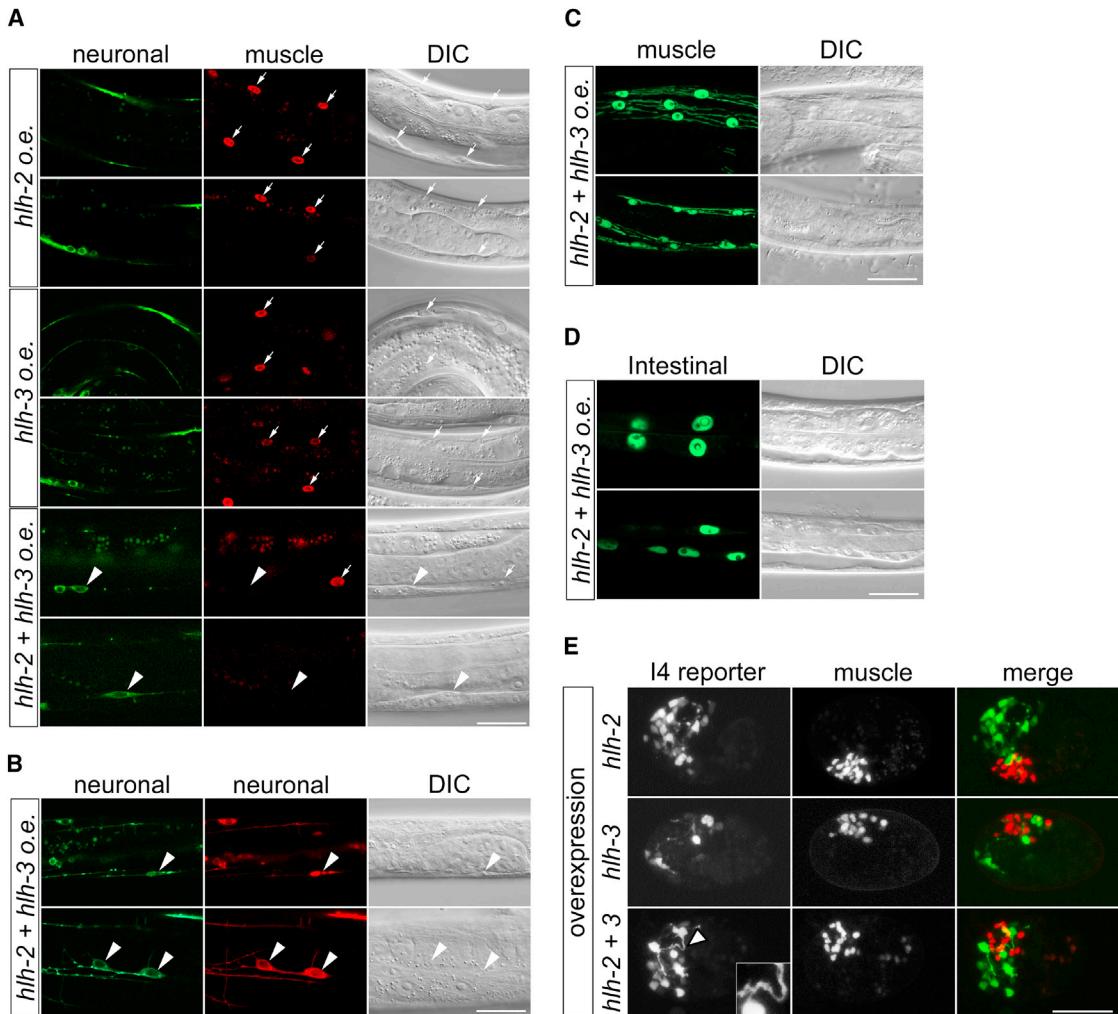
Figure 6. bHLH Overexpression Induces Neuronal Cell-Fate Transformation of Non-neuronal Cells

(A) Confocal images of heat-shocked transgenic animals showing ectopic expression after HLH-2 and HLH-3 coexpression of the neuronal reporter $P_{rab-3}::gfp::rab-3$ (arrowheads), but not of the muscle reporter in body-wall muscle nuclei identified by Nomarski and labeled by $P_{myo-3}::mCherry::H2B$ in the wild-type (arrows).

(B) HLH-2 and HLH-3 overexpression induces ectopic expression of a second neuronal reporter, $P_{rgef-1}::dsRed$ (red), in addition to $P_{rab-3}::gfp::rab-3$ (green) in both body-wall muscle nuclei (upper row, arrowheads) and hypodermal cells (lower row, arrowheads).

(C and D) After HLH-2 and HLH-3 co-overexpression, only normal expression patterns are seen for (C) the muscle reporter $P_{myo-3}::gfp$ and (D) the intestinal reporter $P_{elt-2}::gfp$ in heat-shocked animals.

(E) Co-overexpression of HLH-2 and HLH-3 or HLH-2 alone in early embryos induces formation of multiple cells expressing the I4 reporter but does not eliminate muscle reporter expression. The presence of HLH-3 appears to promote complex neurite formation (arrowhead and inset). I4 reporter, $P_{nlp-13}::gfp$; muscle reporter, $P_{myo-2}::mCherry::H2B$.

Two representative animals are shown for each experiment, except in (E). Scale bars, 20 μm.

DISCUSSION

Our current understanding of neurogenesis during metazoan development is based primarily on studies of ectoderm-derived neurons; little is known about how non-ectodermal cells can generate neurons in vivo. Previous studies of a natural epithelial (ectodermal)-to-neuron transdifferentiation in *C. elegans*, Y to PDA, identified the conserved pluripotent factor SOX-2, histone-modifying complexes, and Notch signaling as important components for the reprogramming [50–52]. All of these factors seem to be dispensable for I4 neurogenesis (Figure S6).

HLH-2 and Mediator Cooperate with HLH-3 to Promote Efficient Neurogenesis from Mesoderm

In this study, we analyzed *C. elegans* mutants in which the pharyngeal I4 neuron adopts a muscle cell fate and identified the molecular genetic basis of I4 neurogenesis from mesoderm.

We found that HLH-2 and Mediator, both of which are broadly expressed [22] (Figure 4C), cooperate with more restrictedly expressed HLH-3 to drive efficient neurogenesis of the I4 neuron. The kinase activity of the Mediator kinase module subunit CDK-8 is required for efficient I4 neurogenesis, and CDK-8 possibly acts by inhibiting cyclin H CYH-1 and CDK-7. We
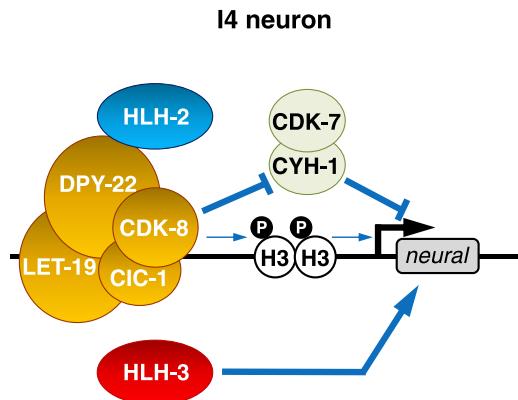
I4 neuron

Figure 7. Model

The HLH-2 proneural protein and the CDK-8 Mediator complex kinase module act with the HLH-3 proneural protein to promote I4 neurogenesis. HLH-2 and CDK-8 most likely act by inhibiting the CYH-1/CDK-7 complex and might also act secondarily by phosphorylating serine 10 of histone H3. CYH-1/CDK-7 might negatively regulate I4 neurogenesis by promoting a myogenic program, whereas H3S10 phosphorylation might facilitate neurogenic gene expression.

speculate that CYH-1 and CDK-7 initiate a myogenic program and that phosphorylation of CYH-1 by CDK-8 inhibits muscle differentiation (Figure 7). It is interesting that despite their ability to form dimers [21], HLH-2 and HLH-3 appear to function in parallel to promote I4 neurogenesis. We speculate that in an HLH-3-deficient mutant, HLH-2 forms homodimers to promote neural gene expression in an HLH-3-independent manner. Given the important role of Ascl1 in promoting neuronal reprogramming of various non-ectodermal cells [53], we hypothesize that HLH-2/Tcf3 and the CDK-8 kinase complex are candidates to enhance Ascl1-mediated mammalian neuronal reprogramming. In addition, because we found that CDK-8 possibly acts by inhibiting CDK-7 and CYH-1 cyclin H, we suggest that small-molecule inhibitors of CDK-7 might similarly promote neurogenesis.

bHLH Proneural Proteins Are Required for Neurogenesis from Both Ectodermal and Non-ectodermal Cells

bHLH proneural proteins are evolutionarily conserved transcription factors that consist of multiple families, including achaete-scute (Asc), atonal (Ato), neurogenin, and neuroD, all of which are evolutionarily conserved in their role of promoting neurogenesis [54, 55]. We found that HLH-3/Ascl1 is expressed specifically in I4 and is needed for I4 to express a neuronal cell fate (Figure 2), and the proneural proteins neurogenin NGN-1 and neuroD CND-1 promote neurogenesis of the M1 and I3 neurons from mesoderm, respectively (Figures S3C and S3D). These findings indicate that proneural proteins are important for driving neurogenesis from both ectoderm and mesoderm. Consistent with this notion, the jellyfish atonal-like gene *Atl1* is expressed in proliferating neural precursor cells arising from striated muscles during transdifferentiation [56], and mammalian bone marrow stromal cells that can be induced to form neurons express the proneural protein NeuroD [57]. We propose that evolutionarily conserved bHLH proneural proteins are important for neurogenesis whatever the germ-layer origin of the neuron. Unlike ecto-

dermal neurons, non-ectodermal neurons might also require additional proteins, such as Mediator, to promote highly efficient neurogenesis.

Natural Non-ectodermal Neurogenesis Might Be a General Aspect of Animal Development

At least three animals are known to generate neurons from non-ectodermal origins: the sea urchin, which generates some pharyngeal neurons de novo from endoderm [1]; the jellyfish (hydrozoan medusa), which generates peptidergic neural cells from striated muscle [2]; and *C. elegans*, which generates neurons from mesodermal MS lineages [3]. Non-ectodermal neurogenesis has been observed in these species because they have simple anatomies and are mostly transparent, allowing high-resolution cell-lineage tracing. Vertebrates also have the potential for a germ layer to generate cells that are conventionally thought to be derived from another germ layer. For example, mice generate paraxial mesodermal cells from ectodermal neural plate in a process dependent on the T box transcription factor Tbx6 [58]. Similarly, avian ectodermal neural crest cells can give rise to multiple mesodermal tissues [59]. Conversely, mesoderm-derived bone marrow stromal cells can differentiate into neurons under certain conditions in vitro, although it remains unclear whether this process occurs naturally during mammalian development [60]. Thus, although the generation of neurons from non-ectodermal cells has yet to be reported in more complex animals, advances in methodology for cell-lineage tracing might lead to the identification of such events in the near future.

EXPERIMENTAL PROCEDURES

Mutagenesis Screen

oxIs322; nIs310 L4 larvae were mutagenized with ethyl methanesulfonate as described previously [61]. See the Supplemental Experimental Procedures for details.

Microscopy

Nomarski differential interference contrast (DIC) and epifluorescence images were obtained using an Axioskop 2 (Zeiss) compound microscope and Open-LAB software (Agilent) and edited using Photoshop CS4 software (Adobe). For tracing embryonic lineages, two- or four-cell-stage embryos were dissected from gravid hermaphrodites and mounted on a slide with a 5% agarose pad. The embryonic lineages were determined by direct observation of cell divisions, and images were taken at appropriate time points. Confocal images were obtained using Zeiss LSM 800 (Figures 6A–6D) and LSM 510 (all other confocal images) microscopes and processed in Fiji software (NIH) and Photoshop CS4 software (Adobe).

Laser Microsurgery

Laser-ablation experiments were performed as described previously. In brief, two-cell-stage embryos were dissected from gravid hermaphrodites and mounted on a slide with a 2% agarose pad. The embryos were allowed to divide to generate P2 and E cells, and laser ablation [62] of AB, P2, and E was performed. Embryos were recovered, grown at 22°C overnight, and examined using a compound microscope for GFP reporter expression.

Full methods are described in the Supplemental Experimental Procedures.

SUPPLEMENTAL INFORMATION

Supplemental Information includes Supplemental Experimental Procedures and six figures and can be found with this article online at http://dx.doi.org/10.1016/j.cub.2017.01.056.

REFERENCES

1. Wei, Z., Angerer, R.C., and Angerer, L.M. (2011). Direct development of neurons within foregut endoderm of sea urchin embryos. Proc. Natl. Acad. Sci. USA *108*, 9143–9147.

2. Seipel, K., and Schmid, V. (2005). Evolution of striated muscle: jellyfish and the origin of triploblasty. Dev. Biol. *282*, 14–26.

3. Sulston, J.E., Schierenberg, E., White, J.G., and Thomson, J.N. (1983). The embryonic cell lineage of the nematode *Caenorhabditis elegans*. Dev. Biol. *100*, 64–119.

4. Okkema, P.G., Ha, E., Haun, C., Chen, W., and Fire, A. (1997). The *Caenorhabditis elegans* NK-2 homeobox gene *ceh-22* activates pharyngeal muscle gene expression in combination with *pha-1* and is required for normal pharyngeal development. Development *124*, 3965–3973.

5. Haun, C., Alexander, J., Stainier, D.Y., and Okkema, P.G. (1998). Rescue of *Caenorhabditis elegans* pharyngeal development by a vertebrate heart specification gene. Proc. Natl. Acad. Sci. USA *95*, 5072–5075.

6. Caiazzo, M., Dell'Anno, M.T., Dvoretskova, E., Lazarevic, D., Taverna, S., Leo, D., Sotnikova, T.D., Menegon, A., Roncaglia, P., Colciago, G., et al. (2011). Direct generation of functional dopaminergic neurons from mouse and human fibroblasts. Nature *476*, 224–227.

7. Son, E.Y., Ichida, J.K., Wainger, B.J., Toma, J.S., Rafuse, V.F., Woolf, C.J., and Eggan, K. (2011). Conversion of mouse and human fibroblasts into functional spinal motor neurons. Cell Stem Cell *9*, 205–218.

8. Vierbuchen, T., Ostermeier, A., Pang, Z.P., Kokubu, Y., Südhof, T.C., and Wernig, M. (2010). Direct conversion of fibroblasts to functional neurons by defined factors. Nature *463*, 1035–1041.

9. Mahoney, T.R., Liu, Q., Itoh, T., Luo, S., Hadwiger, G., Vincent, R., Wang, Z.-W., Fukuda, M., and Nonet, M.L. (2006). Regulation of synaptic transmission by RAB-3 and RAB-27 in *Caenorhabditis elegans*. Mol. Biol. Cell *17*, 2617–2625.

10. Bénard, C., Tjoe, N., Boulin, T., Recio, J., and Hobert, O. (2009). The small, secreted immunoglobulin protein ZIG-3 maintains axon position in *Caenorhabditis elegans*. Genetics *183*, 917–927.

11. Stefanakis, N., Carrera, I., and Hobert, O. (2015). Regulatory logic of pan-neuronal gene expression in *C. elegans*. Neuron *87*, 733–750.

12. Rauthan, M., Mörck, C., and Pilon, M. (2007). The *C. elegans* M3 neuron guides the growth cone of its sister cell M2 via the Krüppel-like zinc finger protein MNM-2. Dev. Biol. *311*, 185–199.

13. Frøkjaer-Jensen, C., Davis, M.W., Hopkins, C.E., Newman, B.J., Thummel, J.M., Olesen, S.-P., Grunnet, M., and Jorgensen, E.M. (2008). Single-copy insertion of transgenes in *Caenorhabditis elegans*. Nat. Genet. *40*, 1375–1383.

14. Cabrera, C.V., Martinez-Arias, A., and Bate, M. (1987). The expression of three members of the achaete-scute gene complex correlates with neuroblast segregation in *Drosophila*. Cell *50*, 425–433.

15. Guillemot, F., Lo, L.C., Johnson, J.E., Auerbach, A., Anderson, D.J., and Joyner, A.L. (1993). Mammalian achaete-scute homolog 1 is required for the early development of olfactory and autonomic neurons. Cell *75*, 463–476.

16. Marro, S., Pang, Z.P., Yang, N., Tsai, M.-C., Qu, K., Chang, H.Y., Südhof, T.C., and Wernig, M. (2011). Direct lineage conversion of terminally differentiated hepatocytes to functional neurons. Cell Stem Cell *9*, 374–382.

17. Okkema, P.G., Harrison, S.W., Plunger, V., Aryana, A., and Fire, A. (1993). Sequence requirements for myosin gene expression and regulation in *Caenorhabditis elegans*. Genetics *135*, 385–404.

18. Culetto, E., Combes, D., Fedon, Y., Roig, A., Toutant, J.P., and Arpagaus, M. (1999). Structure and promoter activity of the 5′ flanking region of *ace-1*, the gene encoding acetylcholinesterase of class A in *Caenorhabditis elegans*. J. Mol. Biol. *290*, 951–966.

19. Serrano-Saiz, E., Poole, R.J., Felton, T., Zhang, F., De La Cruz, E.D., and Hobert, O. (2013). Modular control of glutamatergic neuronal identity in *C. elegans* by distinct homeodomain proteins. Cell *155*, 659–673.

20. Casarosa, S., Fode, C., and Guillemot, F. (1999). Mash1 regulates neurogenesis in the ventral telencephalon. Development *126*, 525–534.

21. Grove, C.A., De Masi, F., Barrasa, M.I., Newburger, D.E., Alkema, M.J., Bulyk, M.L., and Walhout, A.J. (2009). A multiparameter network reveals extensive divergence between *C. elegans* bHLH transcription factors. Cell *138*, 314–327.

22. Krause, M., Park, M., Zhang, J.M., Yuan, J., Harfe, B., Xu, S.Q., Greenwald, I., Cole, M., Paterson, B., and Fire, A. (1997). A *C. elegans* E/Daughterless bHLH protein marks neuronal but not striated muscle development. Development *124*, 2179–2189.

23. Caudy, M., Grell, E.H., Dambly-Chaudière, C., Ghysen, A., Jan, L.Y., and Jan, Y.N. (1988). The maternal sex determination gene daughterless has zygotic activity necessary for the formation of peripheral neurons in *Drosophila*. Genes Dev. *2*, 843–852.

24. Merrill, B.J., Pasolli, H.A., Polak, L., Rendl, M., García-García, M.J., Anderson, K.V., and Fuchs, E. (2004). Tcf3: a transcriptional regulator of axis induction in the early embryo. Development *131*, 263–274.

25. Kim, C.H., Oda, T., Itoh, M., Jiang, D., Artinger, K.B., Chandrasekharappa, S.C., Driever, W., and Chitnis, A.B. (2000). Repressor activity of Headless/Tcf3 is essential for vertebrate head formation. Nature *407*, 913–916.

26. Nakano, S., Ellis, R.E., and Horvitz, H.R. (2010). Otx-dependent expression of proneural bHLH genes establishes a neuronal bilateral asymmetry in *C. elegans*. Development *137*, 4017–4027.

27. Yin, J.W., and Wang, G. (2014). The Mediator complex: a master coordinator of transcription and cell lineage development. Development *141*, 977–987.

28. Malik, S., and Roeder, R.G. (2010). The metazoan Mediator co-activator complex as an integrative hub for transcriptional regulation. Nat. Rev. Genet. *11*, 761–772.

29. Bourbon, H.M., Aguilera, A., Ansari, A.Z., Asturias, F.J., Berk, A.J., Bjorklund, S., Blackwell, T.K., Borggrefe, T., Carey, M., Carlson, M., et al. (2004). A unified nomenclature for protein subunits of Mediator complexes linking transcriptional regulators to RNA polymerase II. Mol. Cell *14*, 553–557.

30. Hong, S.-K., Haldin, C.E., Lawson, N.D., Weinstein, B.M., Dawid, I.B., and Hukriede, N.A. (2005). The zebrafish kohtalo/trap230 gene is required for the development of the brain, neural crest, and pronephric kidney. Proc. Natl. Acad. Sci. USA *102*, 18473–18478.

31. Rocha, P.P., Scholze, M., Bleiss, W., and Schrewe, H. (2010). Med12 is essential for early mouse development and for canonical Wnt and Wnt/PCP signaling. Development *137*, 2723–2731.

32. Shin, C.H., Chung, W.S., Hong, S.K., Ober, E.A., Verkade, H., Field, H.A., Huisken, J., and Stainier, D.Y. (2008). Multiple roles for Med12 in vertebrate endoderm development. Dev. Biol. *317*, 467–479.

33. Esposito, G., Di Schiavi, E., Bergamasco, C., and Bazzicalupo, P. (2007). Efficient and cell specific knock-down of gene function in targeted *C. elegans* neurons. Gene *395*, 170–176.

34. Ding, N., Zhou, H., Esteve, P.-O., Chin, H.G., Kim, S., Xu, X., Joseph, S.M., Friez, M.J., Schwartz, C.E., Pradhan, S., and Boyer, T.G. (2008). Mediator links epigenetic silencing of neuronal gene expression with X-linked mental retardation. Mol. Cell *31*, 347–359.

35. Zhou, R., Bonneaud, N., Yuan, C.X., de Santa Barbara, P., Boizet, B., Tibor, S., Scherer, G., Roeder, R.G., Poulat, F., and Berta, P. (2002). SOX9 interacts with a component of the human thyroid hormone receptor-associated protein complex. Nucleic Acids Res. *30*, 3245–3252.

36. Massari, M.E., Jennings, P.A., and Murre, C. (1996). The AD1 transactivation domain of E2A contains a highly conserved helix which is required for its activity in both *Saccharomyces cerevisiae* and mammalian cells. Mol. Cell. Biol. *16*, 121–129.

37. Zarifi, I., Kiparaki, M., Koumbanakis, K.A., Giagtzoglou, N., Zacharioudaki, E., Alexiadis, A., Livadaras, I., and Delidakis, C. (2012). Essential roles of Da transactivation domains in neurogenesis and in E(spl)-mediated repression. Mol. Cell. Biol. *32*, 4534–4548.

38. Kapoor, A., Goldberg, M.S., Cumberland, L.K., Ratnakumar, K., Segura, M.F., Emanuel, P.O., Menendez, S., Vardabasso, C., Leroy, G., Vidal, C.I., et al. (2010). The histone variant macroH2A suppresses melanoma progression through regulation of CDK8. Nature *468*, 1105–1109.

39. Firestein, R., Bass, A.J., Kim, S.Y., Dunn, I.F., Silver, S.J., Guney, I., Freed, E., Ligon, A.H., Vena, N., Ogino, S., et al. (2008). CDK8 is a colorectal cancer oncogene that regulates beta-catenin activity. Nature *455*, 547–551.

40. Knuesel, M.T., Meyer, K.D., Donner, A.J., Espinosa, J.M., and Taatjes, D.J. (2009). The human CDK8 subcomplex is a histone kinase that requires Med12 for activity and can function independently of Mediator. Mol. Cell. Biol. *29*, 650–661.

41. Meyer, K.D., Donner, A.J., Knuesel, M.T., York, A.G., Espinosa, J.M., and Taatjes, D.J. (2008). Cooperative activity of cdk8 and GCN5L within Mediator directs tandem phosphoacetylation of histone H3. EMBO J. *27*, 1447–1457.

42. Fryer, C.J., White, J.B., and Jones, K.A. (2004). Mastermind recruits CycC:CDK8 to phosphorylate the Notch ICD and coordinate activation with turnover. Mol. Cell *16*, 509–520.

43. Deng, H., Bao, X., Cai, W., Blacketer, M.J., Belmont, A.S., Girton, J., Johansen, J., and Johansen, K.M. (2008). Ectopic histone H3S10 phosphorylation causes chromatin structure remodeling in *Drosophila*. Development *135*, 699–705.

44. Fischle, W., Tseng, B.S., Dormann, H.L., Ueberheide, B.M., Garcia, B.A., Shabanowitz, J., Hunt, D.F., Funabiki, H., and Allis, C.D. (2005). Regulation of HP1-chromatin binding by histone H3 methylation and phosphorylation. Nature *438*, 1116–1122.

45. Hirota, T., Lipp, J.J., Toh, B.-H., and Peters, J.-M. (2005). Histone H3 serine 10 phosphorylation by Aurora B causes HP1 dissociation from heterochromatin. Nature *438*, 1176–1180.

46. Akoulitchev, S., Chuikov, S., and Reinberg, D. (2000). TFIIH is negatively regulated by cdk8-containing Mediator complexes. Nature *407*, 102–106.

47. Garrett, S., Barton, W.A., Knights, R., Jin, P., Morgan, D.O., and Fisher, R.P. (2001). Reciprocal activation by cyclin-dependent kinases 2 and 7 is directed by substrate specificity determinants outside the T loop. Mol. Cell. Biol. *21*, 88–99.

48. Link, C.D., Cypser, J.R., Johnson, C.J., and Johnson, T.E. (1999). Direct observation of stress response in *Caenorhabditis elegans* using a reporter transgene. Cell Stress Chaperones *4*, 235–242.

49. Tursun, B., Patel, T., Kratsios, P., and Hobert, O. (2011). Direct conversion of *C. elegans* germ cells into specific neuron types. Science *331*, 304–308.

50. Kagias, K., Ahier, A., Fischer, N., and Jarriault, S. (2012). Members of the NODE (Nanog and Oct4-associated deacetylase) complex and SOX-2 promote the initiation of a natural cellular reprogramming event in vivo. Proc. Natl. Acad. Sci. USA *109*, 6596–6601.

51. Richard, J.P., Zuryn, S., Fischer, N., Pavet, V., Vaucamps, N., and Jarriault, S. (2011). Direct in vivo cellular reprogramming involves transition through discrete, non-pluripotent steps. Development *138*, 1483–1492.

52. Zuryn, S., Ahier, A., Portoso, M., White, E.R., Morin, M.C., Margueron, R., and Jarriault, S. (2014). Transdifferentiation. Sequential histone-modifying activities determine the robustness of transdifferentiation. Science *345*, 826–829.

53. Amamoto, R., and Arlotta, P. (2014). Development-inspired reprogramming of the mammalian central nervous system. Science *343*, 1239882.

54. Bertrand, N., Castro, D.S., and Guillemot, F. (2002). Proneural genes and the specification of neural cell types. Nat. Rev. Neurosci. *3*, 517–530.

55. Huang, C., Chan, J.A., and Schuurmans, C. (2014). Proneural bHLH genes in development and disease. Curr. Top. Dev. Biol. *110*, 75–127.

56. Seipel, K., Yanze, N., and Schmid, V. (2004). Developmental and evolutionary aspects of the basic helix-loop-helix transcription factors Atonal-like 1 and Achaete-scute homolog 2 in the jellyfish. Dev. Biol. *269*, 331–345.

57. Woodbury, D., Reynolds, K., and Black, I.B. (2002). Adult bone marrow stromal stem cells express germline, ectodermal, endodermal, and mesodermal genes prior to neurogenesis. J. Neurosci. Res. *69*, 908–917.

58. Takemoto, T., Uchikawa, M., Yoshida, M., Bell, D.M., Lovell-Badge, R., Papaioannou, V.E., and Kondoh, H. (2011). Tbx6-dependent Sox2 regulation determines neural or mesodermal fate in axial stem cells. Nature *470*, 394–398.

59. Le Douarin, N.M., Creuzet, S., Couly, G., and Dupin, E. (2004). Neural crest cell plasticity and its limits. Development *131*, 4637–4650.

60. Bianco, P., Riminucci, M., Gronthos, S., and Robey, P.G. (2001). Bone marrow stromal stem cells: nature, biology, and potential applications. Stem Cells *19*, 180–192.

61. Brenner, S. (1974). The genetics of *Caenorhabditis elegans*. Genetics *77*, 71–94.

62. Avery, L., and Horvitz, H.R. (1987). A cell that dies during wild-type *C. elegans* development can function as a neuron in a *ced-3* mutant. Cell *51*, 1071–1078.

Supplemental Information

The CDK8 Complex and Proneural Proteins Together

Drive Neurogenesis from a Mesodermal Lineage

Shuo Luo and H. Robert Horvitz

A

Genotype[a]	% I4-to-muscle transformation	n
hlh-3(n5564)	26	100
hlh-3; Ex[hlh-3(+)]_1	1	100
hlh-3; Ex[hlh-3(+)]_2	0	100
hlh-3; Ex[hlh-3(+)]_3	2	70
let-19(n5470)	19	300
let-19; Ex[let-19(+)]_1	3	100
let-19; Ex[let-19(+)]_2	0	100
let-19; Ex[let-19(+)]_3	4	100
hlh-3(n5469)	18	100
hlh-3; dpy-22(n5572)	62.5	200
hlh-3; dpy-22; Ex[dpy-22(+)]_1	20	50
hlh-3; dpy-22; Ex[dpy-22(+)]_2	19.7	66
hlh-3; dpy-22; Ex[dpy-22(+)]_3	17.5	40

a: Contain oxIs322[Pmyo-2::mCh::H2B] and nIs310[Pnlp-13::gfp].

B
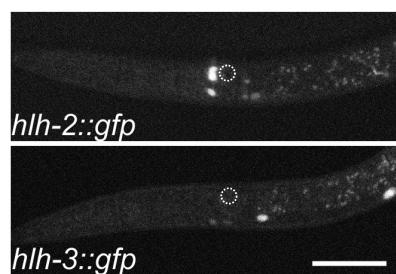
C
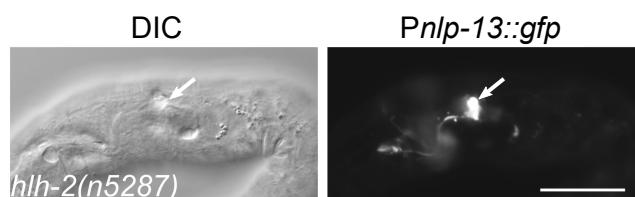
Figure S1. HLH proneural transcription factors and Mediator subunits promote I4 neurogenesis, and HLH proteins likely function in early embryogenesis. Related to Figures 1 and 2. (A) Extrachromosomal array containing hlh-3, let-19 or dpy-22 genomic sequence rescues I4 misspecification phenotype of hlh-3, let-19 or dpy-22 mutants, respectively. (B) Z-projection of the confocal images of L1 transgenic animals expressing either HLH-3::GFP or HLH-2::GFP fusion protein. The position of I4 is marked by the circle. No HLH-3 or HLH-2 expression is observed in the I4 neuron in newly hatched animals, suggesting that HLH proteins function in early embryogenesis to promote I4 development. (C) An arrested homozygous hlh-2 mutant embryo expresses I4 GFP normally (arrows), suggesting a possible maternal contribution of HLH-2 to normal I4 neuronal cell-fate specification. Scale bar, 20 μm.

A

Neurotransmitter	Reporter gene	No. neurons expressing the reporter
Acetylcholine(Ach)	*unc-17*	~120
Glutamate(Glu)	*eat-4*	78
GABA	*unc-25, unc-47*	26
Serotonin(5HT)	*tph-1*	6
Dopamine(DA)	*cat-2*	8
Tyramine(TA)/Octopamine(OA)	*tdc-1*	4

B
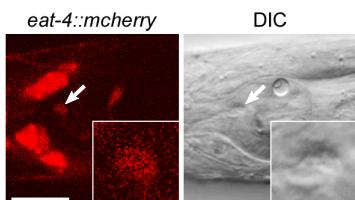
eat-4::mcherry   DIC

C

MS-derived neurons	Neurotransmitter	Reporter transgene	Neurogenesis
I3	Unknown	N/A	+
I4	Glutamate[a]	*eat-4::mCherry*	-
I6	Glutamate[a]	*eat-4::mCherry*	+
M1	Acetylcholine	P*unc-17::gfp*	+
M4	Acetylcholine	P*unc-17::gfp*	+
M5	Glutamate	*eat-4::mCherry*	+

a: Reporter transgene expression variable. See legend.
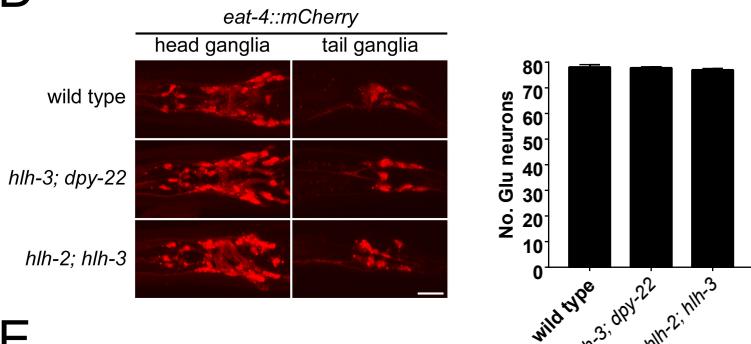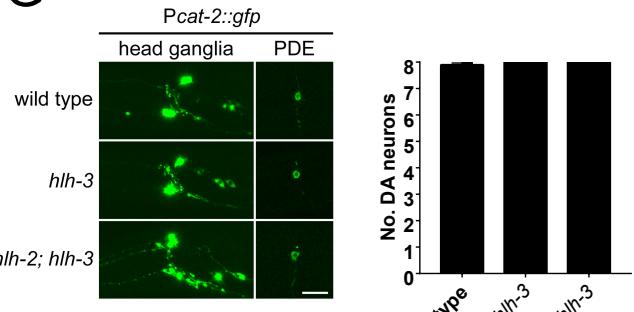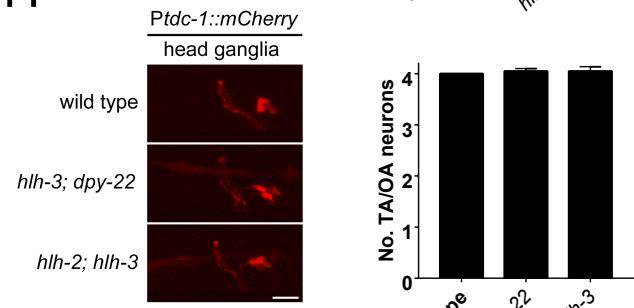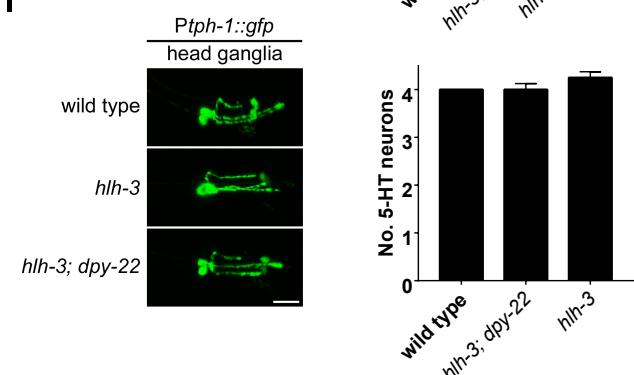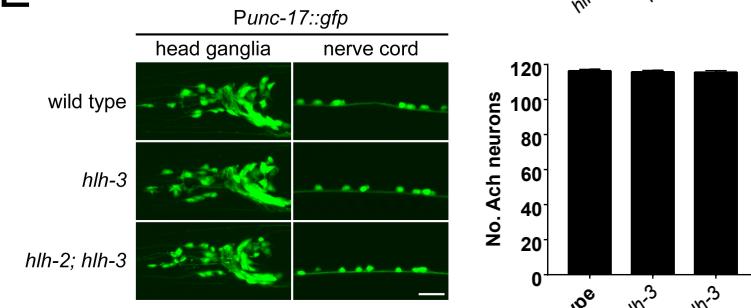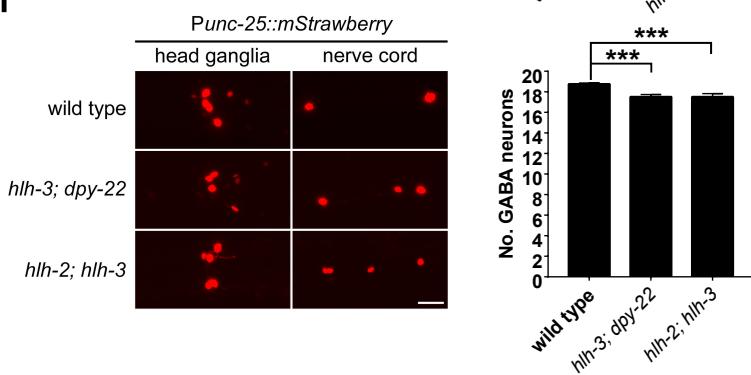
Figure S2. HLH-3 is mostly dispensable for neurogenesis. Related to Figure 2. (A) List of the neurotransmitter reporter transgenes used to examine neurogenesis in *hlh-3* mutants. (B) The I4 neuron expresses a reporter transgene for the glutamate transporter EAT-4 and might be glutamatergic (arrows and insets). (C) The other five MS-derived neurons are generated normally in *hlh-3(n5469)* mutant animals (*n*=40). The glutamatergic reporter transgene P*eat-4*::*eat-4::mCherry* is expressed in I4 and I6 in only 10% (for I4) and 60% (for I6) of the wild-type animals examined. (D-I) HLH-3 and Mediator specifically promote I4 neurogenesis and are likely dispensable for most ectodermal neurogenesis. The generation of (D) glutamatergic (wild type: 78.1 ± 1.0, *n*=10; *hlh-2; hlh-3*: 77.0 ± 0.6, *n*=16; *hlh-3; dpy-22*: 77.8 ± 0.4, *n*=15), (E) cholinergic (wild type: 116.3 ± 0.9, *n*=13; *hlh-2; hlh-3*: 115.5 ± 1.0, *n*=15; *hlh-3; dpy-22*: 115.7 ± 0.9, *n*=17), (G) dopaminergic (wild type: 7.9 ± 0.1, *n*=19; *hlh-3*: 8.0 ± 0, *n*=20; *hlh-2; hlh-3*: 8.0 ± 0, *n*=19), (H) tyraminergic/octopaminergic (wild type: 4.0 ± 0, *n*=20; *hlh-2; hlh-3*: 4.0 ± 0.1, *n*=20; *hlh-3; dpy-22*: 4.0 ± 0.1, *n*=20), and (I) serotonergic (wild type: 4.0 ± 0, *n*=20; *hlh-3; dpy-22*: 4.0 ± 0.1, *n*=20; *hlh-3*: 4.2 ± 0.1, *n*=20) neurons is normal in *hlh-3* single and double mutants. The generation of (F) GABAergic (wild type: 18.8 ± 0.1, *n*=25; *hlh-2; hlh-3*: 17.5 ± 0.3, *n*=25; *hlh-3; dpy-22*: 17.5 ± 0.2, *n*=25, P<0.001) neurons in *hlh-3* double mutants is mildly reduced. We were unable to examine cholinergic neurons in *hlh-3; dpy-22* double mutants, because the cholinergic reporter transgene is tightly linked to *dpy-22*. In (I) we did not score the serotonergic HSN neurons, which are generated but fail to differentiate normally in *hlh-3* mutants and do not express the P*tph-1*::*gfp* reporter transgene [S1]. The slightly higher numbers of serotonergic neurons in *hlh-3* mutants result from partial defects in the cell deaths of the sister cells of the serotonergic NSM neurons [S2] (I). All data represent mean ± s.e.m. ***, P<0.001 by student's t-test. Scale bars, 20 μm.

A

HLH-4, HLH-6, HLH-3, HLH-8, NGN-1, HLH-10, HND-1, HLH-2, HLH-13, CND-1, HLH-14, LIN-32, HLH-12, HLH-19, HLH-15

B
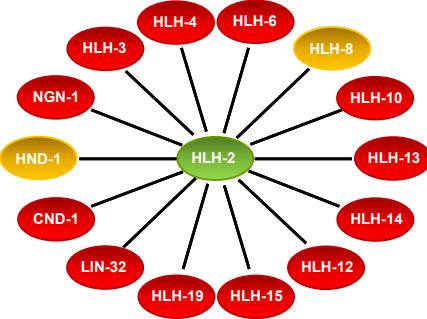
Genotype	% I4-to-muscle transformation	n
wild type[a]	0	100
cnd-1(gk781)[a]	0	200
cnd-1(gk718)[a]	0	200
ngn-1(ok2200)[a]	0	200
hlh-2(bx115); cnd-1(gk718)[b]	0	100
hlh-2(bx115); ngn-1(ok2200)[b]	0	200

a: Contains oxIs322[Pmyo-2::mCherry::h2b] and nIs310[Pnlp-13::gfp]
b: Contains nIs310[Pnlp-13::gfp]

C
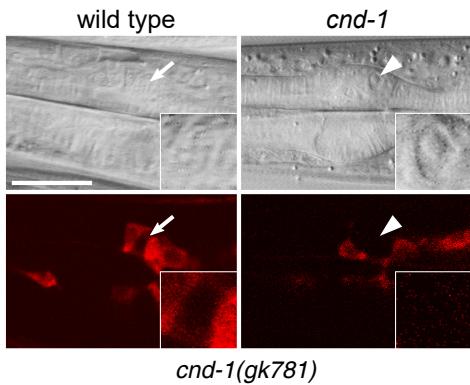
wild type / cnd-1

cnd-1(gk781)

Neuron (%)	I3	I4	I6	M1	M4	M5
wild type	75	100	100	98	100	85
missing	**25**	0	0	0	0	0
mislocalization	0	0	0	2	0	15

Contains otIs173[Prgef-1::dsRed], n=65

D
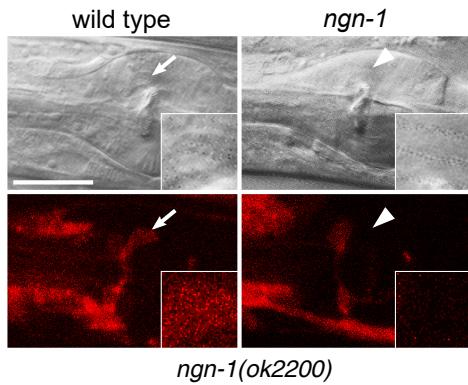
wild type / ngn-1

ngn-1(ok2200)

Neuron (%)	I3	I4	I6	M1	M4	M5
wild type	100	78	96	49	100	98
missing	0	0	0	**41**	0	0
mislocalization	0	22	4	10	0	2

Contains otIs173[Prgef-1::dsRed], n=51

E

lin-32(e1926)

Neuron (%)	I3	I4	I6	M1	M4	M5
wild type	100	100	100	100	100	98
missing	0	0	0	0	0	0
mislocalization	0	0	0	0	0	2

Contains otIs173[Prgef-1::dsRed], n=65

F

hlh-4(tm604)

Neuron (%)	I3	I4	I6	M1	M4	M5
wild type	100	100	96	100	100	96
missing	0	0	0	0	0	0
mislocalization	0	0	4	0	0	4

n=51

G

hlh-6(tm299)

Neuron (%)	I3	I4	I6	M1	M4	M5
wild type	100	100	100	100	100	100
missing	0	0	0	0	0	0
mislocalization	0	0	0	0	0	0

Contains otIs173[Prgef-1::dsRed], n=50

H

hlh-10(ok516)

Neuron (%)	I3	I4	I6	M1	M4	M5
wild type	100	100	100	100	100	100
missing	0	0	0	0	0	0
mislocalization	0	0	0	0	0	0

Contains otIs173[Prgef-1::dsRed], n=51

I

hlh-12(ok1532)

Neuron (%)	I3	I4	I6	M1	M4	M5
wild type	100	100	100	100	100	97
missing	0	0	0	0	0	0
mislocalization	0	0	0	0	0	3

Contains otIs173[Prgef-1::dsRed], n=60

J

hlh-13(tm2279)

Neuron (%)	I3	I4	I6	M1	M4	M5
wild type	100	98	98	100	100	98
missing	0	0	0	0	0	0
mislocalization	0	2	2	0	0	2

Contains otIs173[Prgef-1::dsRed], n=50

K

hlh-15(tm1824)

Neuron (%)	I3	I4	I6	M1	M4	M5
wild type	100	100	100	100	100	98
missing	0	0	0	0	0	0
mislocalization	0	0	0	0	0	2

Contains otIs173[Prgef-1::dsRed], n=50

L

hlh-19(tm3105)

Neuron (%)	I3	I4	I6	M1	M4	M5
wild type	100	100	100	100	98	98
missing	0	0	0	0	0	0
mislocalization	0	0	0	0	2	2

Contains otIs173[Prgef-1::dsRed], n=49

Figure S3. Multiple bHLH proteins are required for neurogenesis of MS neurons. Related to Figure 2. (A) Diagram adopted from [S3] showing the *C. elegans* bHLH proteins known to interact with HLH-2. The bHLH proteins involved in muscle but not neuronal development are shown in orange. (B) Disruption of proneural proteins NGN-1 or CND-1 does not result in I4 misspecification nor does it enhance I4 misspecification in *hlh-2* mutants. (C) Confocal images showing the transformation of the I3 neuron (wild type, arrows and insets) into a non-neuronal cell (arrowheads and insets) and the quantification of I3 neurogenesis defects in *cnd-1* mutants. (D) Confocal images showing the absence of the M1 neuron (wild type, arrows and insets) in *ngn-1* mutants (arrowheads and insets) and the quantification of M1 neurogenesis defects in *ngn-1* mutants. (E-L) The generation of MS-derived neurons is grossly normal in bHLH mutants (E) *lin-32*, (F) *hlh-4*, (G) *hlh-6*, (H) *hlh-10*, (I) *hlh-12*, (J) *hlh-13*, (K) *hlh-15*, and (L) *hlh-19*. Scale bar, 20 μm.

A

Genotype	% I4-to-muscle transformation	n	Other defects
wild type[a]	0	100	
let-19(n5470)[a]	14	900	
let-19(n5563)[a]	9	600	
let-19(ok331)[b]	5	55	Unc Egl Pvl
dpy-22(n5571)[a]	8	400	
dpy-22(n5572)[a]	15	300	
dpy-22(n5573)[a]	11	500	
dpy-22(n5574)[a]	10	500	
dpy-22(n5662)[a]	10	400	
dpy-22(e652)	16	43	Dpy Unc Gro Egl
dpy-22(bx92)[c]	12	34	
dpy-22(sy622)[d]	6.5	200	Dpy Unc Gro Egl

a. Contains oxIs322[Pmyo-2::mCh::H2B] and nIs310[Pnlp-13::gfp]
b. Homozygous mutant progeny of let-19 (ok331)/+ mother were scored
c. Contains pal-5(e2091) and him-5(e1490)
d. Contains nIs310[Pnlp-13::gfp]

B

| Genotype[a]	% I4-to-muscle transformation	n	Other defects
Vector(RNAi)	0	200	
dpy-22(RNAi)	2	200	
dpy-22(n5572); vector(RNAi)	3	100	
dpy-22(n5572); dpy-22(RNAi)	2	100	
let-19(RNAi)	1	200	
let-19(n5470); vector(RNAi)	6	100	
let-19(n5470); let-19(RNAi)	19	177	Gro Ste Emb

a: Contains oxIs322[Pmyo-2::mCherry::h2b] and nIs310[Pnlp-13::gfp]

C

D
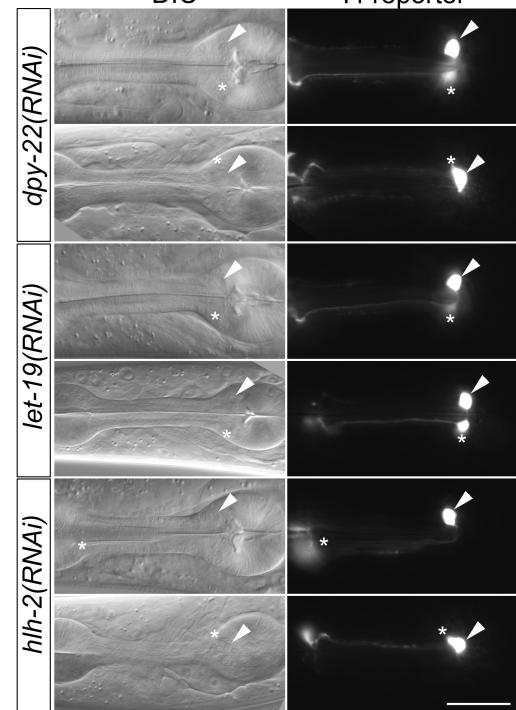
Genotype[a]	% I4-to-muscle transformation	n
Ex[Pnlp-13::let-19(RNAi)]	0	100
Ex[Pnlp-13::dpy-22(RNAi)]	0	100
Ex[Pnlp-13::hlh-2(RNAi)]	0	100

a: Contain oxIs322[Pmyo-2::mCherry::H2B] and nIs310[Pnlp-13::gfp].

Figure S4. Disruption of the Mediator subunits LET-19 and DPY-22 leads to I4 misspecification. Related to Figure 3. (A) The *dpy-22* and *let-19* alleles examined cause incomplete penetrances of I4 misspecification. (B) Further reduction of DPY-22 or LET-19 function by RNAi in *dpy-22* or *let-19* mutants does not significantly enhance I4 misspecification. (C) Cell-specific RNAi by expressing coding fragments of *dpy-22*, *let-19*, or *hlh-2* under the *nlp-13* promoter in late embryos does not disrupt I4 specification. The positions of I4 and M2 are marked by arrowheads and asterisks, respectively. I4 reporter, $P_{nlp-13}::gfp$. (D) Quantification of cell-specific RNAi. Scale bar, 20 μm.

A

CDK-8

D182A, kinase dead

N 1 ▼ 588 C

tm1238

CIC-1

N 1 302 C

tm3740

100 a.a.

B

Genotype	% I4-to-muscle transformation	n	Other defects
wild type[a]	0	100	
dpy-22(n5572)[a]	3	100	
let-19(n5470)[a]	11	100	
hlh-2(bx115)[b]	0	100	
cdk-8(tm1238)[a]	1	100	Dpy
cic-1(tm3740)[a]	1	100	Dpy
cdk-8(tm1238); dpy-22(n5572)[a]	13	300	Dpy Egl
cic-1(tm3740); dpy-22(n5572)[a]	7	100	Dpy Egl
cdk-8(tm1238); let-19(n5470)[a]	N.D.	N.D.	Let
let-19(n5470); cic-1(tm3740)[a]	N.D.	N.D.	Let
hlh-2(bx115) cdk-8(tm1238)[b]	2	200	Dpy
hlh-2(bx115); cic-1(tm3740)[b]	1	300	Dpy

a: Contains oxIs322[Pmyo-2::mCherry::h2b] and nIs310[Pnlp-13::gfp]
b: Contains nIs310[Pnlp-13::gfp]

C

cdk-8(tm1238); cnd-1(gk781)

Neuron (%)	I3	I4	I6	M1	M4	M5
wild type	78	98	100	100	98	100
missing	22	0	0	0	0	0
mislocalization	0	2	0	0	2	0

Contains otIs173[Prgef-1::dsRed], n=55

D

cdk-8(tm1238); ngn-1(ok2200)

Neuron (%)	I3	I4	I6	M1	M4	M5
wild type	100	87	98	40	100	93
missing	0	0	0	45	0	0
mislocalization	0	13	2	15	0	7

Contains otIs173[Prgef-1::dsRed], n=60

E

cdk-8; hlh-3

wild type / hlh-3 / cdk-8 / cdk-8; hlh-3 / WT cdk-8 rescue / KD cdk-8 rescue

anti-H3S10P
anti-H3
anti-H3T3P
anti-H3
anti-H3K9me3
anti-H3

F

% I4-to-muscle transformation

wild type / hlh-3(n5469) / cdk-8(tm1238) / cdk-8; hlh-3 / cdk-8; hlh-3; H3.3S10D o.e. / cdk-8; hlh-3; H3.1S10D o.e.

*** 0.39 *** ***

Figure S5. CDK-8 functions together with Mediator and in parallel to HLH-3 to promote I4 neurogenesis. Related to Figure 5. (A) Schematics showing the protein domains of CDK-8 and CIC-1 and the molecular lesions of specified *cdk-8* and *cic-1* alleles. (B) Introducing the *cdk-8* or *cic-1* allele into Mediator or *hlh-2* mutants does not enhance I4 misspecification, suggesting that CDK-8 and CIC-1 function in the same pathway as Mediator and HLH-2 to promote I4 neurogenesis. Dpy, dumpy; Egl, egg-laying defective; Emb, embryonic lethal; Gro, slow growing; Let, lethal; Pvl, protruding vulva; Ste, sterile; Unc, uncoordinated; N.D., not determined. (C) *cdk-8; cnd-1* double mutants have I3 misspecification similar to that of *cnd-1* single mutant (compared to Fig. S3C). (D) *cdk-8; ngn-1* double mutants have M1 misspecification similar to that of *ngn-1* single mutant (compared to Fig. S3D). (E) Western blot showing significantly reduced H3S10 phosphorylation in *cdk-8; hlh-3* double mutants; this reduced phosphorylation is rescued by wild-type (WT) but not kinase-dead (KD) CDK-8 overexpression. H3T3 phosphorylation and H3K9me3 levels remain unaffected. The significant global decrease in H3S10 phosphorylation might be a result of synergistic effects of *cdk-8* and *hlh-3* single mutants, as *hlh-3* mutant animals likely have higher serotonin levels because of the presence of extra serotonergic NSM-like neurons ([S2], Fig. S2I legend), and both serotonin and the CDK8 complex have been implicated in stress responses in metazoa [S4–7]. H3S10 phosphorylation has been shown to be sensitive to stress response [S8,S9] and thus could be more significantly affected in *cdk-8; hlh-3* double mutants. The blot is representative of two biological repeats. (F) Overexpression of a phosphomimetic His3.3 protein HIS-71 but not of His3.1 protein HIS-9 using the native histone promoter partially suppresses I4 misspecification in *cdk-8; hlh-3* double mutants. n=100-400 for three independent experiments. Data represent mean ± s.e.m.. ***, P<0.001 by student's t-test.

A

egl-27(ok1670)

Neuron (%)	I3	I4	I6	M1	M4	M5
wild type	100	100	100	100	100	88
missing	0	0	0	0	0	0
mislocalization	0	0	0	0	0	12

n=40

B

sem-4(n1971)

Neuron (%)	I3	I4	I6	M1	M4	M5
wild type	100	100	100	100	100	100
missing	0	0	0	0	0	0
mislocalization	0	0	0	0	0	0

n=40

C

Genotype[a]	% I4-to-muscle transformation	*n*
Vector(RNAi)	0	200
egl-27(RNAi)	0	200
sem-4(RNAi)	0	200
ceh-6(RNAi)	0	200
sox-2(RNAi)_clone1	0	200
sox-2(RNAi)_clone2	0	200
set-2(RNAi)	0	200
set-16(RNAi)	1.5	200
ash-2(RNAi)	0	200
wdr-5.1(RNAi)	0	200
rbbp-5(RNAi)	0	200
jmjd-3.1(RNAi)	0	200
cfp-1(RNAi)	0	200
dpy-30(RNAi)	0	200

a: Contains *oxIs322[Pmyo-2::mCh::H2B]* and *nIs310[Pnlp-13::gfp]*.

D

Genotype[a]	% I4-to-muscle transformation	*n*
hlh-3(n5469); Vector(RNAi)	9	200
hlh-3(n5469); egl-27(RNAi)	10.5	200
hlh-3(n5469); sem-4(RNAi)	11	200
hlh-3(n5469); ceh-6(RNAi)	13.5	200
hlh-3(n5469); sox-2(RNAi)_clone1	14	200
hlh-3(n5469); sox-2(RNAi)_clone2	12	200
hlh-3(n5469); set-2(RNAi)	10	200
hlh-3(n5469); set-16(RNAi)	40	200
hlh-3(n5469); ash-2(RNAi)	8	200
hlh-3(n5469); wdr-5.1(RNAi)	10	200
hlh-3(n5469); rbbp-5(RNAi)	10.5	200
hlh-3(n5469); jmjd-3.1(RNAi)	11	200
hlh-3(n5469); cfp-1(RNAi)	6	200
hlh-3(n5469); dpy-30(RNAi)	15	200

a: Contains *oxIs322[Pmyo-2::mCh::H2B]* and *nIs310[Pnlp-13::gfp]*.

E

lin-12(n137sd)

Neuron (%)	I3	I4	I6	M1	M4	M5
wild type	100	100	100	100	100	98
missing	0	0	0	0	0	0
mislocalization	0	0	0	0	0	2

n=45

F

lin-12(n941)

Neuron (%)	I3	I4	I6	M1	M4	M5
wild type	100	100	92	98	100	92
missing	0	0	0	0	0	0
mislocalization	0	0	8	2	0	8

n=40

G

Genotype[a]	% I4-to-muscle transformation	*n*	Note
wild type	0	200	
lin-12(RNAi)	0	200	
glp-1(RNAi)	0	200	
lag-1(RNAi)	0	30	Emb, Lva
hlh-3(n5469)	14	100	
hlh-3; lin-12(RNAi)	11.5	200	
hlh-3; glp-1(RNAi)	10	200	
hlh-3; lag-1(RNAi)	N/A	N/A	Emb
cdk-8(tm1238); hlh-3(n5469)	42	200	Dpy, Egl
cdk-8; hlh-3; lin-12(RNAi)	37	200	
cdk-8; hlh-3; glp-1(RNAi)	37.5	8	Emb, Ste

a: Contains *oxIs322[Pmyo-2::mCh::H2B]* and *nIs310[Pnlp-13::gfp]*.

Figure S6. Factors required for Y-to-PDA transdifferentiation are dispensable for I4 neurogenesis. Related to Figure 5. (A, B) In the Y-to-PDA (epithelial-to-neuron) mutants (A) *egl-27(ok1670)* and (B) *sem-4(n1971)*, the mesoderm-derived neurons I3, I4, I6, M1, M4, and M5 are generated normally. (C, D) RNAi knockdown of the genes involved in the Y-to-PDA transdifferentiation does not induce or enhance I4 misspecification in (C) wild-type or (D) *hlh-3* mutant animals. By contrast, RNAi of the H3K4 methyltransferase gene *set-16* (which is not involved in Y-to-PDA transdifferentiation) significantly enhances I4 neurogenesis defects in *hlh-3* mutants, suggesting that Y-to-PDA transdifferentiation and I4 neurogenesis depend on distinct molecular pathways. (E, F) Notch signaling required for Y-to-PDA transdifferentiation is likely dispensable for I4 neurogenesis. In the gain- and loss-of-function Notch mutants (E) *lin-12(n137sd)* and (F) *lin-12(n941)*, respectively, the mesoderm-derived neurons I3, I4, I6, M1, M4, and M5 are generated normally. (G) RNAi knockdown of the Notch genes *lin-12*, *glp-1* or *lag-1* does not significantly affect I4 neurogenesis in wild-type, *hlh-3* or *cdk-8; hlh-3* mutant animals. Dpy, dumpy; Egl, egg-laying defective; Emb, embryonic lethal; Lva, larval arrest; Ste, sterile; N/A, not assayed.

Supplemental Experimental Procedures

Strains. All *C. elegans* strains were handled and maintained at 22°C as described previously [S10] unless noted otherwise. We used the Bristol strain N2 as the wild-type strain. The mutations used are listed below:

LGI: *ccIs4251[P$_{myo-3}$::gfp(NLS)::LacZ, P$_{myo-3}$::gfp(mitochondrially targeted), dpy-20(+)], cdk-8(tm1238), hlh-2(bx115, n5287, tm1768ts), sem-4(n1971).*

LGII: *egl-27(ok1670), hlh-3(n5469, n5564, n5566, ot354, tm1688), hlh-6(tm299), let-19(n5470, n5563, ok331), oxIs322[P$_{myo-2}$::mCherry::H2B, P$_{myo-3}$::mCherry::H2B, Cbr-unc-119(+)].*

LGIII: *cic-1(tm3740), cnd-1(gk718, gk781), hlh-4(tm604), jsIs682[P$_{rab-3}$::gfp::rab-3, lin-15(+)], lin-12(n137sd, n941), otIs173[P$_{rgef-1}$::dsRed2, P$_{ttx-3}$::gfp], nIs695[P$_{ceh-22}$::ceh-22::mCherry, P$_{pgp-12}$::mCherry].*

LGIV: *hlh-12(ok1532), ngn-1(ok2200), bcIs25[P$_{tph-1}$::gfp, lin-15(+)], nIs198[P$_{unc-25}$::mStrawberry, lin-15(+)], nIs407[P$_{hlh-2}$::hlh-2::gfp, lin-15(+)], nIs756[P$_{his-9}$::his-9(S10D), P$_{unc-54}$::mCherry].*

LGV: *hlh-10(ok516), kyIs405[P$_{elt-2}$::elt-2::GFP], nIs310[P$_{nlp-13}$::gfp, lin-15(+)], nIs662[P$_{hlh-3}$::hlh-3::gfp, P$_{unc-54}$::mCherry], otIs292[P$_{eat-4}$::eat-4::mCherry, rol-6(su1006)], nIs757[P$_{his-71}$::his-71(S10D), P$_{unc-54}$::mCherry].*

LGX: *dpy-22(bx92, e652, n5571, n5572, n5573, n5574, n5662, sy622), hlh-13(tm2279), hlh-15(tm1824), hlh-19(tm3105), lin-32(e1926), nIs116[P$_{cat-2}$::gfp, lin-15(+)], vsIs48[P$_{unc-17}$::gfp].*

unknown linkage: *nIs324[P$_{tdc-1}$::mStrawberry, lin-15(+)], nIs625[P$_{dpy-22}$::gfp], nIs626[P$_{let-19}$::gfp], nIs656 [P$_{hsp-16.2}$::hlh-2(cDNA), rol-6(su1006)], nIs657[P$_{hsp-16.2}$::hlh-3(cDNA), rol-6(su1006)], nIs658[P$_{hsp-16.2}$::hlh-2(cDNA), P$_{hsp-16.2}$::hlh-3(cDNA), rol-6(su1006)], stIs10089[P$_{hlh-1}$::his-24::mCherry, unc-119(+)].*

Extrachromosomal arrays: *nEx2343[P$_{ace-1}$::mCherry], nEx2227[P$_{dpy-22}$::cdk-8(cDNA)::dpy-22 3'-UTR, P$_{unc-54}$::mCherry], nEx2228[P$_{dpy-22}$::cdk-8(cDNA, KD)::dpy-22 3'-UTR, P$_{unc-54}$::mCherry], nEx2554[P$_{dpy-22}$::cyh-1(S5D S327D, cDNA)::dpy-22 3'-UTR, P$_{unc-54}$::mCherry], nEx2555[P$_{dpy-22}$::cyh-1(S5A S327A, cDNA)::dpy-22 3'-UTR, P$_{unc-54}$::mCherry], nEx2557[P$_{dpy-22}$::cdk-7(K34A, cDNA)::dpy-22 3'-UTR, P$_{unc-54}$::mCherry], nEx2558[P$_{dpy-22}$::cdk-7(S157E T163E, cDNA)::dpy-22 3'-UTR, P$_{unc-54}$::mCherry].*

Mutagenesis screen. oxIs322; nIs310 L4 larvae were mutagenized with ethyl methanesulfonate (EMS) as described previously [S10]. About 200,000 F2 or F3 animals were screened non-clonally using a dissecting microscope equipped with UV light. Animals that lacked expression of GFP in the I4 cell, which is stereotypically located in the dorsal side of the posterior bulb of the pharynx in wild-type animals, were picked to single Petri plates. The mutant phenotype was verified by fluorescence and Nomarski DIC imaging using a Zeiss Axioskop2 compound microscope equipped with differential interference contrast (DIC) optics. The I4 cell in mutants was identified based on the position of the I4 nucleus relative to its neighboring pharyngeal cells pm5, pm6, I6 and M1. The presence of an extra muscle-like cell that expressed P$_{myo-2}$::mCherry::H2B also aided the identification of the mutant I4 cell. All of the mutants we described are viable as homozygotes.

Molecular biology and fluorescence reporters. The P$_{cat-2}$::gfp, P$_{myo-2}$::mCherry::H2B, P$_{myo-3}$::gfp(NLS)::LacZ, P$_{myo-3}$::gfp(mitochondrially targeted), P$_{rgef-1}$::dsRed2, P$_{unc-17}$::gfp, P$_{tph-1}$::gfp transcriptional reporters and the P$_{eat-4}$::eat-4::mCherry, P$_{elt-2}$::elt-2::gfp, P$_{rab-3}$::gfp::rab-3, P$_{hlh-2}$::hlh-2::gfp translational reporters have been described previously [S2,S11–19].

The P$_{nlp-13}$::gfp transcriptional reporter was constructed by PCR-amplifying a 2.3 kb *nlp-13* promoter fragment with the oligonucleotides fw-GCGCATGcacctttaaaggcgcacgga and rv-GCCTGCAGCGTTGCATgttggaaccctgga. The resulting product was digested by *Sph*I and *Pst*I and cloned into pPD95.75 (kindly provided by A. Fire) digested by the same restriction enzymes. The plasmid was subsequently injected into the germline of *lin-15(n765)* animals to generate transgenic strains.

The P$_{unc-25}$::mStrawberry transcriptional reporter was made by PCR-amplification using the two primers fw-cgaatttttgcatgcaaaaaacacccacttttgatc and rv-CGGGATCCTCgagcacagcatcactttcgtcagcagc. The resulting PCR product was digested by *Sph*I and *Bam*HI and cloned into pSN199 digested by the same enzymes. pSN199 is a derivative of pPD122.56 (kindly provided by A. Fire) carrying mStrawberry instead of GFP. In short, pSN199 was made by replacing GFP of pPD122.56 with mStraberry from the plasmid mStrawberry 6 (a gift from H. Schwartz). GFP and mStrawberry were swapped using *Age*I and *Eco*RI digestion. The plasmid was subsequently injected into the germline of *lin-15(n765)* animals to generate transgenic strains.

The P$_{ceh-22}$::ceh-22::mCherry and P$_{hlh-3}$::hlh-3::gfp translational reporters were constructed using fosmid recombineering as described [S20]. Briefly, *mCherry* or *egfp* coding sequence was amplified from the plasmid

NM1845 pR6KmCherry (kindly provided by M. Nonet) or NM1835 pR6KGFP [S20], respectively, using the oligonucleotides
fw-GACCTTCAGCAGCTTCTTCCTACATGACCAATACTCAATGGTGGCCTTCTGAATTCATGGTGAGCAAGGGC,
rv-GAGATGTATTCTGGGAAAAATTGACATGGTATAGAGTATTAGAGAAATCAaccggcagatcgtcagtcag
(P*dpy-22*::ceh-22::mCherry), and
fw-CATCCACTTCTGGTGATCATCATAGCTTTTATTCGCATACAGAAACTTATagctcaggaggtagcggCA,
rv-CACCCGATTATTTGAGAAAAACAGAAAATATGGTACAACTTAACAGATTAaccggcagatcgtcagtcag
(P*hlh-3*::hlh-3::gfp). The PCR products were digested with *Dpn*I to remove template DNA, gel-purified using a QIAquick gel extraction kit (Qiagen), and 1 µl of the purified products were electroporated into L-rhamnose-induced competent bacterial cells that harbored the helper plasmid pREDFlp4 and the fosmid containing full-length *ceh-22* (fosmid 19b10) or *hlh-3* (fosmid 40n18) genomic DNA. Successful recombinants with *mCherry* or *egfp* recombined into the fosmid were selected by kanamycin resistance, with the *kan^r* gene subsequently removed by anhydrotetracycline-induced Flp recombination. The correct insertion of *mCherry* or *eGFP* was verified by sequencing. The fosmids were subsequently injected into the germline of wild-type animals to generate transgenic strains.

The P*dpy-22*::gfp transcriptional reporter was generated by overlap extension PCR that fused 2 kb *dpy-22* promoter with the 0.7 kb *egfp* sequence from NM1847 pR6KKanRGFP (kindly provided by M. Nonet), followed by 1 kb *dpy-22* 3'-UTR, using the oligonucleotides fw-ccacagcaaattcaaacatttcttg,
rv-ATGGTGGCGACCGGTGCCATACGTTCGCCGGGCTGCTCGT (P*dpy-22*),
fw-ACGAGCAGCCCGGCGAACGTATGGCACCGGTCGCCACCAT,
rv-GAAAGAATATAAATATGTAATTGTGACATGAttaTCCGCGGCCGTCCTTGT (*egfp*),
fw-ACAAGGACGGCCGCGGAtaaTCATGTCACAATTACATATTTATATTCTTTC, and
rv-gcaggtggtacacataggaaag (*dpy-22* 3'-UTR). The PCR product was gel-purified using a QIAquick gel extraction kit and subsequently injected into the germline of wild-type animals to generate transgenic strains.

The P*let-19*::gfp transcriptional reporter was generated by overlap extension PCR that fused a 1.8 kb *let-19* promoter with the 0.7 kb *egfp* sequence from NM1847 pR6KKanRGFP, followed by 1.1 kb *let-19* 3'-UTR, using the oligonucleotides fw-cgagaatgaacaaaaggtttcttc,
rv-ATGGTGGCGACCGGTGCCATGTCCTCTGTGGAGTCACGGG (P*let-19*),
fw-CCCGTGACTCCACAGAGGACATGGCACCGGTCGCCACCAT,
rv-GTACATTTGAAAATTTGATTCACGATATGCttaTCCGCGGCCGTCCTTGT (*egfp*),
fw-ACAAGGACGGCCGCGGAtaaGCATATCGTGAATCAAATTTTCAAATGTAC, and
rv- TGCAGATTCGGACGAAATTGGG (*let-19* 3'-UTR). The PCR product was gel-purified using a QIAquick gel extraction kit and subsequently injected into the germline of wild-type animals to generate transgenic strains.

The P*ace-1*::mCherry transcriptional reporter was generated by overlap extension PCR that fused a 2 kb *ace-1* promoter with the 0.9 kb *mCherry* sequence from pAA64 (kindly provided by K. Oegema), followed by 1.3 kb *unc-54* 3'-UTR from pPD122.56 (kindly provided by A. Fire), using the oligonucleotides fw-ggaagaagaagcagagaagaaa, rv-CTTCTTCACCCTTTGAGACCATGCTTCTTCAACAAATCATAATCGTTTG (P*ace-1*), fw-GATTATGATTTGTTGAAGAAGCATGGTCTCAAAGGGTGAAGAAG,
rv-CTCAGTTGGAATTcTACGAATGCTACTTATACAATTCATCCATGCC (*mCherry*),
fw-GGCATGGATGAATTGTATAAGTAGCATTCGTAgAATTCCAACTGAG, and
rv-GTCTCATGAGCGGATACATATTTG (*unc-54* 3'-UTR). The PCR product was gel-purified using a QIAquick gel extraction kit and subsequently injected into the germline of wild-type animals to generate transgenic strains.

The P*dpy-22*::cdk-8(cDNA, wt or KD)::dpy-22 3'-UTR rescue DNA was generated by overlap extension PCR that fused 2 kb *dpy-22* promoter with the 1.8 kb *cdk-8(wt or KD)* cDNA sequence, followed by 2.2 kb *dpy-22* 3'-UTR, using the oligonucleotides fw-ccacagcaaattcaaacatttcttg,
rv-TCATCAATCATTAATGTCATACGTTCGCCGGGCTGCTCGT (P*dpy-22*),
fw-ACGAGCAGCCCGGCGAACGTATGACATTAATGATTGATGAAAACTTCA,
rv-ATAAATATGTAATTGTGACATGATTATCGATGATATTGTTGTTGCCATTG (*cdk-8*, wt cDNA), or
fw-ACGAGCAGCCCGGCGAACGTATGACATTAATGATTGATGAAAACTTCA,
rv-GATTCTTGAAAATCCCAAAGCAGCAATTTTTACCCT,
fw-AGGGTAAAAATTGCTGCTTTGGGATTTTCAAGAATC,

rv-ATAAATATGTAATTGTGACATGATTATCGATGATATTGTTGTTGCCATTG (*cdk-8*, D182A KD cDNA), and fw-ACAACAATATCATCGATAATCATGTCACAATTACATATTTATATTCTTTC, rv-gatgaggagtgccaaaggataaatg (*dpy-22* 3'-UTR). The PCR products were gel-purified using a QIAquick gel extraction kit and subsequently injected into the germline of wild-type animals to generate transgenic strains.

The 2.4 kb *his-9(S10D)* genomic DNA fragment was generated by PCR-mediated mutagenesis using the oligonucleotides fw-cgctacagcaaacagcaatttaa, rv-TGGAGCCTTTCCTCCGGTGTCTTTACGGGCGGTTTGCTTA (P*his-9*), fw-TAAGCAAACCGCCCGTAAAGACACCGGAGGAAAGGCTCCA, and rv-caatgttttattctctgataaaaagtcaat (*his-9(S10D)*). The PCR product was gel-purified using a QIAquick gel extraction kit and the point mutation was verified by sequencing. It was subsequently injected into the germline of wild-type animals to generate transgenic strains.

The 3.7 kb *his-71(S10D)* genomic DNA fragment was generated by PCR-mediated mutagenesis using the oligonucleotides fw-gtgttgttccctttcattttagc, rv-AGGAGCTTTTCCTCCAGTGTCTTTACGCGCGGTTTGCTTG (P*his-71*), fw-CAAGCAAACCGCGCGTAAAGACACTGGAGGAAAAGCTCCT, and rv-cacacagaaatgcttccaacaaa (*his-71(S10D)*). The PCR product was gel-purified using a QIAquick gel extraction kit and the point mutation was verified by sequencing. It was subsequently injected into the germline of wild-type animals to generate transgenic strains.

The P*dpy-22*::*cyh-1(cDNA, AA)::dpy-22 3'-UTR* rescue DNA was generated by overlap extension PCR that fused 2 kb *dpy-22* promoter with the 1 kb *cyh-1(AA)* cDNA sequence, followed by 2.2 kb *dpy-22* 3'-UTR, using the oligonucleotides fw-ccacagcaaattcaaacatttcttg, rv-TGTGTCGCCGTCGCGTACATACGTTCGCCGGGCTGCTCGT (P*dpy-22*), fw-ACGAGCAGCCCGGCGAACGTATGTACGCGACGGCGACACAAAAACG, rv-GAATATAAATATGTAATTGTGACATGATCAATTAATTTCGTCATCCGCATCAACTGGC (*cyh-1AA*), fw-GCGGATGACGAAATTAATTGATCATGTCACAATTACATATTTATATTCTTTC, and rv-gatgaggagtgccaaaggataaatg (*dpy-22* 3'-UTR). The 5.2 kb final PCR product was gel-purified using a QIAquick gel extraction kit and the point mutations were verified by sequencing. It was subsequently injected into the germline of wild-type animals to generate transgenic strains.

The P*dpy-22*::*cyh-1(cDNA, DD)::dpy-22 3'-UTR* rescue DNA was generated by overlap extension PCR that fused 2 kb *dpy-22* promoter with the 1 kb *cyh-1(DD)* cDNA sequence, followed by 2.2 kb *dpy-22* 3'-UTR, using the oligonucleotides fw-ccacagcaaattcaaacatttcttg, rv-TGTGTGTCCGTCGCGTACATACGTTCGCCGGGCTGCTCGT (P*dpy-22*), fw-ACGAGCAGCCCGGCGAACGTATGTACGCGACGGACACACAAAAACG, rv-GAATATAAATATGTAATTGTGACATGATCAATTAATTTCGTCATCGTCATCAACTGGC (*cyh-1DD*), fw-GACGATGACGAAATTAATTGATCATGTCACAATTACATATTTATATTCTTTC, and rv-gatgaggagtgccaaaggataaatg (*dpy-22* 3'-UTR). The 5.2 kb final PCR product was gel-purified using a QIAquick gel extraction kit and the point mutations were verified by sequencing. It was subsequently injected into the germline of wild-type animals to generate transgenic strains.

The P*dpy-22*::*cdk-7(cDNA, KD)::dpy-22 3'-UTR* rescue DNA was generated by overlap extension PCR that fused 2 kb *dpy-22* promoter with the 1.1 kb *cdk-7(KD)* cDNA sequence, followed by 2.2 kb *dpy-22* 3'-UTR, using the oligonucleotides fw-ccacagcaaattcaaacatttcttg, rv-GTATCGTAACGTCTACTCATACGTTCGCCGGGCTGCTCGT (P*dpy-22*), fw-ACGAGCAGCCCGGCGAACGTATGAGTAGACGTTACGATACAATA, rv-CTCGATCCTAGTTTGATTTTTGCAATAGCCACACATTCGCCCG, fw-CGGGCGAATGTGTGGCTATTGCAAAAATCAAACTAGGATCGAGAGAA, rv-ATAAATATGTAATTGTGACATGATTAATCAAAATTCAATCGTCGAACGG (*cdk-7KD*), fw-GACGATTGAATTTTGATTAATCATGTCACAATTACATATTTATATTCTTTC, and rv-gatgaggagtgccaaaggataaatg (*dpy-22* 3'-UTR). The 5.3 kb final PCR product was gel-purified using a QIAquick gel extraction kit and the point mutation was verified by sequencing. It was subsequently injected into the germline of wild-type animals to generate transgenic strains.

The P*dpy-22*::*cdk-7(cDNA, EE)::dpy-22 3'-UTR* rescue DNA was generated by overlap extension PCR that fused 2 kb *dpy-22* promoter with the 1.1 kb *cdk-7(EE)* cDNA sequence, followed by 2.2 kb *dpy-22* 3'-UTR, using the

oligonucleotides fw-ccacagcaaattcaaacatttcttg,
rv-GTATCGTAACGTCTACTCATACGTTCGCCGGGCTGCTCGT (P*dpy-22*),
fw-ACGAGCAGCCCGGCGAACGTATGAGTAGACGTTACGATACAATA,
rv-ACCTGATG<u>CTC</u>GTAATTTCTGTTTGG<u>CTC</u>TCCGAAGAATCGAGCCAAACC,
fw-TTCTTCGGA<u>GAG</u>CCAAACAGAAATTAC<u>GAG</u>CATCAGGTTGTGACAAGATGGT,
rv-ATAAATATGTAATTGTGACATGATTAATCAAAATTCAATCGTCGAACGG (*cdk-7EE*),
fw-GACGATTGAATTTTGATTAATCATGTCACAATTACATATTTATATTCTTTC, and
rv-gatgaggagtgccaaaggataaatg (*dpy-22* 3'-UTR). The 5.3 kb final PCR product was gel-purified using a QIAquick gel extraction kit and the point mutations were verified by sequencing. It was subsequently injected into the germline of wild-type animals to generate transgenic strains.

The P*hsp-16.2*::*hlh-2(cDNA)* heat-shock plasmid was constructed by amplifying 1.2 kb *hlh-2* cDNA from reverse transcribed first-strand cDNA synthesized from total wild-type RNA (SuperScript III, Invitrogen) using following oligos:
fw-TTGACAGC<u>GCTAGC</u>ATGGCGGATCCAAATAGCCAAC, and
rv-TTGACAGC<u>CCATGG</u>TTAAGCGTAATCTGGTACGTCGTATGGGTAAAACCGTGGATGTCCAAACTGC.
The PCR product was gel purified using a QIAquick gel extraction kit, digested with *Nhe*I, *Nco*I and ligated with the heat-shock vector pPD49.78 (kindly provided by Fire. A). The plasmid was verified by sequencing and was subsequently injected into the germline of wild-type animals to generate transgenic strains.

The P*hsp-16.2*::*hlh-3(cDNA)* heat-shock plasmid was constructed by amplifying 0.5 kb *hlh-3* cDNA from reverse transcribed first-strand cDNA synthesized from total wild-type RNA (SuperScript III, Invitrogen) using following oligos:
fw-TTGACAGC<u>GCTAGC</u>ATGACCGCATCCACCTCCTCA, and
rv-TTGACAGC<u>CCATGG</u>TTAAGCGTAATCTGGTACGTCGTATGGGTAATAAGTTTCTGTATGCGAATAAAAGCT. The PCR product was gel purified using a QIAquick gel extraction kit, digested with *Nhe*I, *Nco*I and ligated with the heat-shock vector pPD49.78 (kindly provided by Fire. A). The plasmid was verified by sequencing and was subsequently injected into the germline of wild-type animals to generate transgenic strains.

The bacterial strains expressing small interfering RNAs that target the following genes either were not available from the Ahringer [S21] or the ORFeome [S22] RNAi library or contained plasmids with incorrect inserts and were constructed as follows. The genomic DNA fragment spanning both exons and introns for *let-19* was amplified using the oligonucleotides fw-TCGC<u>AAGCTT</u>GTCCTCAACTTCAGCTGGAAAT and
rv-AGAG<u>AAGCTT</u>GGAGTTTCCAGTCCAAGATCTT. The PCR product was gel-purified using a QIAquick gel extraction kit, digested with *Hin*dIII, ligated with *Hin*dIII digested RNAi vector pL4440 [S22], and transformed into HT115 *E. coli* cells. All RNAi clones were verified by sequencing.

The tissue-specific RNAi transgenes P*nlp-13*::*dpy-22*, P*nlp-13*::*let-19* and P*nlp-13*::*hlh-2* were constructed by amplifying 2.2 kb sense and antisense gene fragments as well as 2.3 kb *nlp-13* promoter using following oligos:
fw-ccacctttaaaggcgcacgga,
rv-CGAAGGTTGGTTTTCCGGAGGTTGGAACCctggaagaaagaa (P*nlp-13*, sense);
fw-ctttcttccagGGTTCCAACCTCCGGAAAACCAACCTTCGA,
rv-CAGCCATTTCAGCATCGTCAG (*dpy-22*, sense);
fw-ccacctttaaaggcgcacgga,
rv-TGACGATGCTGAAATGGCTGGTTGGAACCctggaagaaagaa (P*nlp-13*, antisense);
fw-ctttcttccagGGTTCCAACCAGCCATTTCAGCATCGTCAG,
rv-CTCCGGAAAACCAACCTTCGA (*dpy-22*, antisense);
fw-ccacctttaaaggcgcacgga,
rv-cagcgcacCTTGGCGGAGGAGTTGGAACCctggaagaaagaa (P*nlp-13*, sense);
fw-ctttcttccagGGTTCCAACTCCTCCGCCAAGgtgcgct,
rv-GACTCCGAATTTTGTGCCATCT (*let-19*, sense);
fw-ccacctttaaaggcgcacgga,
rv-ATGGCACAAAATTCGGAGTCGTTGGAACCctggaagaaagaa (P*nlp-13*, antisense);
fw-ctttcttccagGGTTCCAACGACTCCGAATTTTGTGCCATCT,
rv-TCCTCCGCCAAGgtgcgct (*let-19*, antisense);

fw-ccacctttaaaggcgcacgga,
rv-AGTTGGCTATTTGGATCCGCGTTGGAACCctggaagaaagaa (P$_{nlp-13}$, sense);
fw-ctttcttccagGGTTCCAACGCGGATCCAAATAGCCAACTTA,
rv-CTTTCTCGAGCATTATTCTGTGA (*hlh-2*, sense);
fw-ccacctttaaaggcgcacgga,
rv-CAGAATAATGCTCGAGAAAGGTTGGAACCctggaagaaagaa (P$_{nlp-13}$, antisense);
fw-ctttcttccagGGTTCCAACCTTTCTCGAGCATTATTCTGTGA,
rv-GCGGATCCAAATAGCCAACTTA (*hlh-2*, antisense).

The P$_{nlp-13}$::*sense* and P$_{nlp-13}$::*antisense* fragments were generated using overlap PCR, purified and mixed at a final concentration of 5 ng/µl and injected with 5 ng/µl of P$_{unc-54}$::*mCherry* and 100 ng/µl of pcDNA3 into the germline of wild-type animals to generate transgenic strains.

RNAi treatments. RNAi experiments were performed by feeding worms with bacteria expressing small interference RNAs, as described previously [S21,S22]. Briefly, HT115 *E. coli* cells carrying RNAi clones were cultured overnight in LB liquid media supplemented with 75 mg/L ampicillin. 30 µl of bacterial culture were seeded into individual wells of 24-well NGM plates supplemented with 1 mM IPTG and 75 mg/L ampicillin, and the plates were incubated at room temperature (22°C) overnight (>12 hrs) to induce siRNA expression. For RNAi experiments, three to ten L2 larvae were transferred to individual wells of the RNAi plates, grown at room temperature (22°C) for three to four days, and the F1 progeny were scored for I4 GFP expression. Worms that lacked GFP expression specifically in I4 were scored as I4-defective. Bacteria expressing the empty RNAi vector pL4440 were used as a control.

Western blots. Worms were grown on 100 mm plates with *E. coli* OP50 bacterial lawn until the *E. coli* was almost depleted; two plates of worms were harvested for each genotype. Worm pellets were flash-frozen in liquid nitrogen, thawed at room temperature, and resuspended in ice-cold 400 µl (final volume) of 1×SDS lysis buffer (2% SDS, 50 mM Tris pH6.8, 10% glycerol). The suspension was sonicated using a Fisher Scientific Sonicator (Model: FB120, 120W, 20 kHz) at 50% output for 3×5 second pulses with 1 min intervals between pulses. Samples were then boiled at 95°C for 20 min. 15 µg of protein was resolved on a 4-15% Bio-Rad Mini-Protean TGX gel, transferred to a nitrocellulose membrane (Whatman Protran, 0.45 µm) and blotted with anti-phospho-H3S10 antibody (Millipore, 06-570) at 1:2000 dilution. The same membrane was stripped and re-blotted with anti-H3 antibody (Santa Cruz, sc-8654r) at 1:1000 dilution. Signals were developed using Chemiluminescence Reagent Plus Kit (PerkinElmer, NEL105), and images were captured with Bio-Rad ChemiDoc MP imaging system. All images were processed using Adobe Photoshop CS4.

Germline transformation. Transgenic lines were constructed using standard germline transformation procedures [S23]. All DNA samples were injected at a final concentration of 10 ng/µl. We used P$_{unc-54}$::*mCherry* or P$_{pgp-12}$::*4×NLS::mCherry* as a coinjection marker when needed at 5 ng/µl, and we co-injected pcDNA3 at 100 ng/µl for each injection. For non-integrated transgenic lines that carry extrachromosomal arrays, at least two independent lines were analyzed and averages are shown.

Yeast two-hybrid assay. The yeast two-hybrid assay was performed following the manufacturer's protocol (Clontech). Briefly, fresh Yeast Gold colonies (<1 week old) were cultured in YPD liquid medium at 30°C to the O.D.$_{600}$ of 0.5, harvested, washed, and resuspended in 1.1 × TE/LiAc. 100 ng of bait and prey plasmids were mixed with 50 µg of denatured salmon sperm carrier DNA and were transformed into competent yeast cells in the presence of 1× PEG/LiAc. The cell mix was then plated on both –Leu–Trp and –Leu–Trp–His–Ade dropout plates and was allowed to grow at 30°C for 2-3 days. Single colonies that grew on the double and quadruple dropout plates were resuspended in H$_2$O and respotted to fresh dropout plates, which were grown at 30°C for 2 days. Images of the respotted plates were captured using a Canon Powershot A590 digital camera (Canon) and processed by Photoshop CS4 software (Adobe).

Heat shock. To induce HLH-2 and HLH-3 overexpression, L1 larval transgenic animals carrying the P$_{hsp-16.2}$::*hlh-2/3* transgene were picked to a fresh plate spotted with OP50 bacteria and heat-shocked at 34°C for 1 hour. The animals were then placed at 22°C overnight before being examined using a confocal microscope.

Supplemental References

S1.   Doonan, R., Hatzold, J., Raut, S., Conradt, B., and Alfonso, A. (2008). HLH-3 is a *C. elegans* Achaete/Scute protein required for differentiation of the hermaphrodite-specific motor neurons. Mech. Dev. *125*, 883–893.

S2.   Thellmann, M., Hatzold, J., and Conradt, B. (2003). The Snail-like CES-1 protein of *C. elegans* can block the expression of the BH3-only cell-death activator gene *egl-1* by antagonizing the function of bHLH proteins. Development *130*, 4057–4071.

S3.   Grove, C. a, De Masi, F., Barrasa, M.I., Newburger, D.E., Alkema, M.J., Bulyk, M.L., and Walhout, A.J.M. (2009). A multiparameter network reveals extensive divergence between *C. elegans* bHLH transcription factors. Cell *138*, 314–27.

S4.   Chaouloff, F., Berton, O., and Mormède, P. (1999). Serotonin and stress. Neuropsychopharmacology *21*.

S5.   Xie, Y., Moussaif, M., Choi, S., Xu, L., and Sze, J.Y. (2013). RFX transcription factor DAF-19 regulates 5-HT and innate immune responses to pathogenic bacteria in *Caenorhabditis elegans*. PLoS Genet. *9*, e1003324.

S6.   Jin, C., Strich, R., and Cooper, K.F. (2014). Slt2p phosphorylation induces cyclin C nuclear-to-cytoplasmic translocation in response to oxidative stress. Mol. Biol. Cell *25*, 1396–1407.

S7.   Wang, K., Yan, R., Cooper, K.F., and Strich, R. (2015). Cyclin C mediates stress-induced mitochondrial fission and apoptosis. Mol. Biol. Cell *26*, 1030–43.

S8.   Ke, Q., Li, Q., Ellen, T.P., Sun, H., and Costa, M. (2008). Nickel compounds induce phosphorylation of histone H3 at serine 10 by activating JNK-MAPK pathway. Carcinogenesis *29*, 1276–1281.

S9.   Dyson, M.H., Thomson, S., Inagaki, M., Goto, H., Arthur, S.J., Nightingale, K., Iborra, F.J., and Mahadevan, L.C. (2005). MAP kinase-mediated phosphorylation of distinct pools of histone H3 at S10 or S28 via mitogen- and stress-activated kinase 1/2. J. Cell Sci. *118*, 2247–2259.

S10.   Brenner, S. (1974). The genetics of *Caenorhabditis elegans*. Genetics *77*, 71–94.

S11.   Frøkjaer-Jensen, C., Davis, M.W., Hopkins, C.E., Newman, B.J., Thummel, J.M., Olesen, S.-P., Grunnet, M., and Jorgensen, E.M. (2008). Single-copy insertion of transgenes in *Caenorhabditis elegans*. Nat. Genet. *40*, 1375–83.

S12.   Bénard, C., Tjoe, N., Boulin, T., Recio, J., and Hobert, O. (2009). The small, secreted immunoglobulin protein ZIG-3 maintains axon position in *Caenorhabditis elegans*. Genetics *183*, 917–27.

S13.   Mahoney, T.R., Liu, Q., Itoh, T., Luo, S., Hadwiger, G., Vincent, R., Wang, Z.-W., Fukuda, M., and Nonet, M.L. (2006). Regulation of synaptic transmission by RAB-3 and RAB-27 in *Caenorhabditis elegans*. Mol. Biol. Cell *17*, 2617–2625.

S14.   Nakano, S., Ellis, R.E., and Horvitz, H.R. (2010). Otx-dependent expression of proneural bHLH genes establishes a neuronal bilateral asymmetry in *C. elegans*. Development *137*, 4017–27.

S15.   Chase, D.L., Pepper, J.S., and Koelle, M.R. (2004). Mechanism of extrasynaptic dopamine signaling in *Caenorhabditis elegans*. Nat. Neurosci. *7*, 1096–1103.

S16.   Serrano-Saiz, E., Poole, R.J., Felton, T., Zhang, F., De La Cruz, E.D., and Hobert, O. (2013). Modular control of glutamatergic neuronal identity in *C. elegans* by distinct homeodomain proteins. Cell *155*, 659–673.

S17.   Fire, A., Xu, S., Montgomery, M.K., Kostas, S.A., Driver, S.E., and Mello, C.C. (1998). Potent and specific genetic interference by double-stranded RNA in *Caenorhabditis elegans*. Nature *391*, 806–811.

S18.   Lints, R., and Emmons, S.W. (1999). Patterning of dopaminergic neurotransmitter identity among *Caenorhabditis elegans* ray sensory neurons by a TGFbeta family signaling pathway and a Hox gene. Development *126*, 5819–5831.

S19.   Murray, J.I., Bao, Z., Boyle, T.J., Boeck, M.E., Mericle, B.L., Nicholas, T.J., Zhao, Z., Sandel, M.J., and Waterston, R.H. (2008). Automated analysis of embryonic gene expression with cellular resolution in *C. elegans*. Nat. Methods *5*, 703–709.

S20.   Sarov, M., Schneider, S., Pozniakovski, A., Roguev, A., Ernst, S., Zhang, Y., Hyman, a A., and Stewart, a F. (2006). A recombineering pipeline for functional genomics applied to *Caenorhabditis elegans*. Nat. Methods *3*, 839–44.

S21.   Kamath, R.S., Fraser, A.G., Dong, Y., Poulin, G., Durbin, R., Gotta, M., Kanapin, A., Bot, N. Le, Moreno, S., Sohrmann, M., *et al.* (2003). Systematic functional analysis of the *Caenorhabditis elegans* genome using RNAi. Nature *421*, 231–7.

S22.   Rual, J., Ceron, J., Koreth, J., Hao, T., Nicot, A., Hirozane-kishikawa, T., Vandenhaute, J., Orkin, S.H., Hill, D.E., Heuvel, S. Van Den, *et al.* (2004). Toward improving *Caenorhabditis elegans* phenome mapping with an ORFeome-based RNAi library. Genome Res *14*, 2162–8.

S23.   Mello, C., Kramer, J., Stinchcomb, D., and Ambros, V. (1991). Efficient gene transfer in *C.elegans*: extrachromosomal maintenance and integration of transforming sequences. EMBO J. *10*, 3959–3970.